HHS Public Access

Author manuscript

*Cell Rep*. Author manuscript; available in PMC 2024 February 18.

Published in final edited form as:

*Cell Rep*. 2024 January 23; 43(1): 113660. doi:10.1016/j.celrep.2023.113660.

# A comparative evaluation of the strengths and potential caveats of the microglial inducible CreER mouse models

**Alicia M. Bedolla**[1,2], **Gabriel L. McKinsey**[3,4], **Kierra Ware**[1], **Nicolas Santander**[5], **Thomas D. Arnold**[3,4], **Yu Luo**[1,2,6,7,*]

[1]Department of Molecular and Cellular Biosciences, University of Cincinnati, Cincinnati, OH 45229, USA

[2]Neuroscience Graduate Program, University of Cincinnati, Cincinnati, OH 45229, USA

[3]Department of Pediatrics, University of California, San Francisco, San Francisco, CA 94143, USA

[4]Cardiovascular Research Institute, University of California, San Francisco, San Francisco, CA 94158, USA

[5]Instituto de Ciencias de la Salud, Universidad de O'Higgins, Rancagua, Chile

[6]Immunology Graduate Program, Cincinnati Children's Hospital Medical Center

[7]Lead contact

## SUMMARY

The recent proliferation of new *Cre* and *CreER* recombinase lines provides researchers with a diverse toolkit to study microglial gene function. To determine how best to apply these lines in studies of microglial gene function, a thorough and detailed comparison of their properties is needed. Here, we examined four different microglial *CreER* lines (*Cx3cr1*$^{YFP\text{-}CreER(Litt)}$, *Cx3cr1*$^{CreER(Jung)}$, *P2ry12*$^{CreER}$, and *Tmem119*$^{CreER}$), focusing on (1) recombination specificity, (2) leakiness (the degree of tamoxifen-independent recombination in microglia and other cells), (3) the efficiency of tamoxifen-induced recombination, (4) extraneural recombination (the degree of recombination in cells outside of the CNS, particularly myelo/monocyte lineages), and (5) off-target effects in the context of neonatal brain development. We identify important caveats and strengths for these lines, which will provide broad significance for researchers interested in performing conditional gene deletion in microglia. We also provide data emphasizing the potential of these lines for injury models that result in the recruitment of splenic immune cells.



*Correspondence: luoy2@ucmail.uc.edu.

AUTHOR CONTRIBUTIONS

Y.L. and A.B. conceptualized the study. A.B., G.L.M., T.D.A., and Y.L. designed the experiments. A.B. performed most of the *in vitro* and *in vivo* experiments and recorded and analyzed data with help from K.W. G.L.M. carried out part of the neonatal TAM experiment, and N.S. performed the bioinformatic data analysis. A.B., G.L.M., T.D.A., and Y.L. drafted and revised the paper. All authors read, edited, and approved the final version of the manuscript.

SUPPLEMENTAL INFORMATION

Supplemental information can be found online at https://doi.org/10.1016/j.celrep.2023.113660.

DECLARATION OF INTERESTS

The authors declare no competing interests.

## Graphical Abstract

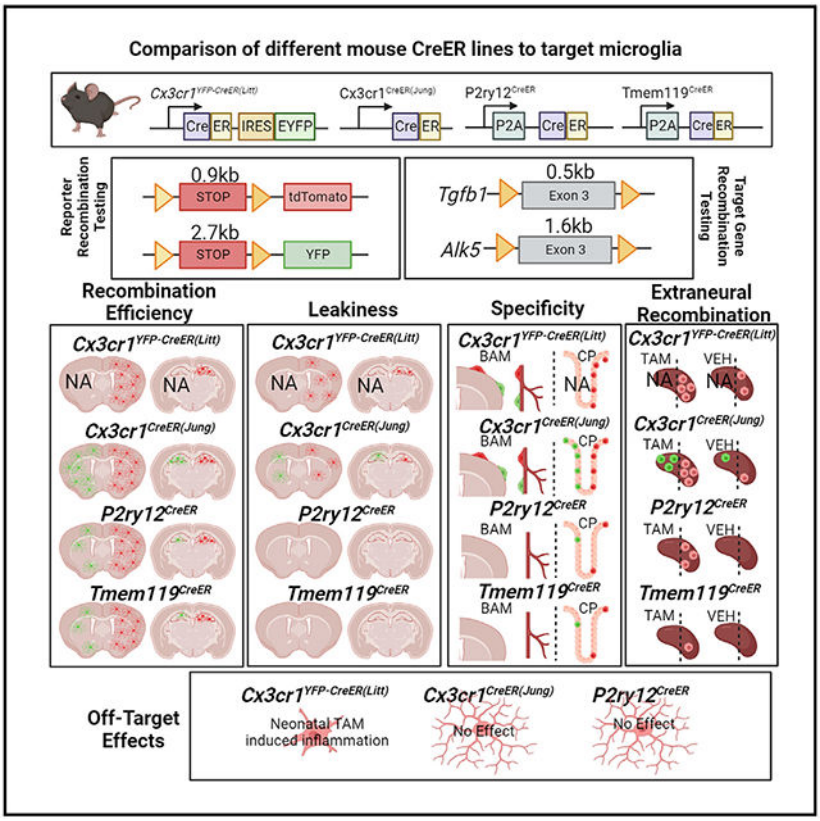


## In brief

Microglia are essential in brain homeostasis. Tools to label and manipulate microglia are vital for understanding their roles. Bedolla et al. characterized recombination specificity, leakiness, efficiency, extraneural/peripheral recombination, and potential off-target effects in 4 publicly available CreER mouse lines in addition to suggestions for future experimental design.

## INTRODUCTION

Microglia, the resident macrophages of the neural parenchyma, regulate a variety of processes necessary for brain development, homeostatic function, and injury/disease response. In addition to their role in innate immunity in the brain and surveillance of parenchyma, during both development and adulthood, microglia have been credited with synaptic pruning, which plays a vital role in synaptic plasticity.[1-4] Outside the realms of development and homeostasis, microglia also respond to disease and injury, with varying activation profiles depending on the challenge.[5,6] With the increase in knowledge and recognition of these processes has come a significant expansion of the number of *Cre* and *CreER* recombinase mouse lines to enable precise genetic targeting of microglia.[7-10] Manipulation of the fractalkine receptor *Cx3cr1* gene locus has been one of the primary methods used to drive *Cre* and *CreER* expression in microglia (reviewed in Wieghofer et al.[11]). *Cx3cr1* is strongly expressed in microglia as well as other myeloid subsets,

providing relatively specific gene targeting. Since their establishment, these lines have been collectively utilized in over 1,000 published reports. These reports highlight the broad utility of *Cx3cr1*-based gene targeting but also describe several potentially important drawbacks, including non-microglia recombination (lack of specificity),[12] leakiness,[13] and off-target effects.[12,14] Based on then-emerging transcriptomic profiling, *Sall1*$^{CreER}$ mice[15] were proposed to be more specific for the genetic manipulation of microglial cells than *Cx3cr1*$^{CreER}$ mice. However, a detailed characterization later found that *Sall1*$^{CreER}$ recombines neural-ectodermal lineages, including neurons, astrocytes, and oligodendrocyte populations, and also has significant tamoxifen-independent (leaky) recombination in microglia.[12] Furthermore, *Sall1*$^{CreER}$ mice, like *Cx3cr1*$^{CreER}$ mice, were generated as a knockin/knockout at the endogenous gene locus. Because *Sall1* is known to be critical for the maintenance of microglial homeostasis and activation,[15,16] heterozygous loss of *Sall1* in *CreER* mice could have important impacts on microglia, complicating interpretation of lineage tracing and gene knockout experiments.

In recent years, several new *CreER* mice were generated to overcome the drawbacks of existing microglia-targeting lines. In particular, *Tmem119*$^{CreER}$ and *P2ry12*$^{CreER}$ lines were generated to have increased specificity for microglia while sparing brain-border macrophages (BAMs), such as perivascular and pial macrophages.[8,10] In addition to this increased specificity, these new lines lack recombination in circulating monocytes, making it easier to distinguish microglia from invading monocytes in the context of injury or disease. With the advent of these new lines, a systematic and direct comparison of their properties is needed. A number of characteristics are of particular interest to researchers when deciding which *CreER* to use for conditional mutagenesis studies, including (1) specificity (which cells in the CNS/brain are recombined by the *CreER*), (2) leakiness (the degree of tamoxifen-independent recombination in microglia and other cells), (3) efficiency (how well *loxP*-flanked DNA regions are recombined in the presence of tamoxifen), (4) extraneural recombination (related to specificity; the degree of recombination in cells outside of the CNS, particularly myelo/monocyte lineages, that can enter the CNS in development or disease); and (5) off-target effects (whether there are unintended effects of gene targeting and/or tamoxifen administration in particular lines). With these five primary characteristics in mind, we performed a rigorous evaluation of four publicly available (The Jackson Laboratories, JAX) microglia-targeting *CreER* lines: *Cx3cr1*$^{YFP–CreER(Litt)}$ (generated by the Littman lab[17]), *Cx3cr1*$^{CreER(Jung)}$ (generated by the Jung lab[18]), *Tmem119*$^{CreER}$,[10] and *P2ry12*$^{CreER}$.[8] We report that there is significant variability across lines in their leakiness and in their ability to recombine floxed alleles, which we show is related both to *loxP* distance and intrinsic *CreER* activity or expression. We describe successful strategies to boost the recombination efficiency using homozygous *P2ry12*$^{CreER}$ mice as well as our unsuccessful efforts to improve recombination efficiency by crossing to the new *iSuRe-Cre* mouse line.[19] We also document significant differences in splenic recombination in the studied *CreER* lines, reflective of potential injury-induced monocyte recruitment from the spleen. In total, these comparative analyses provide important data for research groups eager to determine whether a particular microglial recombining *CreER* line would be appropriate and useful for studies of cell lineage tracing and/or conditional gene mutation in microglia.

## RESULTS

### Different degrees of leakiness in microglia *CreER* lines

We first looked to confirm microglia specificity while also assessing leakiness in *P2ry12*$^{CreER}$ and *Tmem119*$^{CreER}$ mice. We analyzed *Cx3cr1*$^{CreER(Jung)}$ and *Cx3cr1*$^{YFP\text{-}CreER(Litt)}$, both previously well characterized, as baseline controls. For these studies, we took advantage of what is widely regarded as the most sensitive Cre recombinase reporter, *Ai9*, and a less sensitive Cre reporter, *ROSA26-YFP* (hereafter referred to as *R26-YFP*) for comparison. Due to the *Cx3cr1*$^{YFP\text{-}CreER(Litt)}$ line carrying an internal ribosome entry site (IRES)-enhanced yellow fluorescent protein (*EYFP*) gene reporter, we only examined a cross with the *Ai9-tdTomato* reporter in this line as *Cx3cr1*$^{YFP\text{-}CreER(Litt)}$*Ai9*. We assessed both male and female mice treated with tamoxifen (180 mg/kg, daily gavage for 5 days) compared with mice treated with vehicle (sunflower oil + ethanol) kept in separate cages throughout the induction and analysis period (to ensure no tamoxifen contamination). Vehicle treatment provides a control for tamoxifen treatment and also allows an assessment of leakiness—the number and types of cells recombined in the absence of tamoxifen.

As expected, tamoxifen induction in adult *Cx3cr1*$^{YFP\text{-}CreER(Litt)}$ and *Cx3cr1*$^{CreER(Jung)}$ mice resulted in recombination of the *Ai9 tdTomato* Cre-reporter allele in microglia as well as brain-border macrophages in the choroid plexus, meninges, and perivascular spaces (Figures 1, bottom, and S1). In contrast, tamoxifen-treated *Tmem119*$^{CreER}$ and *P2ry12*$^{CreER}$ mice had more specific tdTomato labeling of microglia and no apparent labeling of brain-border macrophages (characterized by anatomical location and expression of LYVE1 and CD206; Figure S1) or other parenchymal neurons and glia (data not shown). *Tmem119*$^{CreER}$ and *P2ry12*$^{CreER}$ both recombine a small subset of IBA1$^{+}$ choroid plexus (ChP) macrophages, including Kolmer's epiplexus cells, which are also targeted by *Cx3cr1*$^{CreER}$ lines (at a higher percentage) (Figure S1). Interestingly, *Tmem119*$^{CreER}$ recombined some Iba1$^{-}$ cells in the choroid plexus, meninges, and around large blood vessels (LYVE1 and reporter double-positive cells), which likely represent brain-border fibroblasts known to strongly express *Tmem119*. Comparing recombination in mice with the *Ai9* versus the *R26-YFP* recombination reporter, we observed significantly fewer recombined IBA1$^{+}$ brain macrophages in *Tmem119*$^{CreER}$ and *P2ry12*$^{CreER}$ lines with *R26-YFP* (94.55% for the *Tmem119*$^{CreER}$*Ai9* mice and 95.81% for the *P2ry12*$^{CreER}$*Ai9* mice vs. 33.78% for *Tmem119*$^{CreER}$*R26-YFP* and 36.51% for *P2ry12*$^{CreER}$*Ai9*) (Figure 1); YFP fluorescence was enhanced when using anti-GFP immunostaining to minimize differences in endogenous fluorescence. This finding was confirmed using fluorescence-activated cell sorting (FACS) analysis (Figure S2). We attribute this difference in Cre reporting to the intrinsic sensitivity of the two Cre recombinase reporters, a function of inter-*loxP* distances (0.9 kb in *Ai9*, 2.7 kb in *R26-YFP*), mRNA-stabilizing elements (*Ai9* has *WRPE*), enhanced promoter elements (*Ai9* uses a strong *CAG* promoter), and native fluorescence intensity (*Ai9* tdT vs. YFP). Similar tamoxifen-induced reporter recombination efficiency in all mouse lines was observed in multiple brain regions (cortex or CTX, striatum or STR, and hippocampus or HC; Figures 1, S3, and S4).

Tamoxifen-independent *Ai9-tdTomato* recombination has been described previously in *Cx3cr1*$^{YFP\text{-}CreER(Litt)}$,[20] *Cx3cr1*$^{CreER(Jung)}$,[12] and *P2ry12*$^{CreER}$[8] lines. Using the *Ai9* Cre reporter, we similarly observed relatively high degrees of tamoxifen-independent recombination in microglia in the two *Cx3cr1*$^{CreER}$ lines (82% and 28%, respectively) and sparse recombination (tdTomato expression) of microglia in *P2ry12*$^{CreER}$*Ai9* and *Tmem119*$^{CreER}$*Ai9* mice in the absence of tamoxifen (Figure 1, top). Interestingly, in the *Cx3cr1*$^{CreER(Jung)}$ line, we observed slightly variable tamoxifen (TAM)-independent "leakiness" in tdTomato recombination at different brain regions (cortex, 28%; striatum, 37%; hippocampus, 47%; Figures 1, S3, and S4). Similar to the *P2ry12*$^{CreER}$*Ai9* mice, we observed sparse non-TAM recombination of microglia in *Tmem119*$^{CreER}$*Ai9* mice. Using the *R26-YFP* reporter line, we observed much less TAM-independent expression of the YFP reporter in the *Cx3cr1*$^{CreER(Jung)}$*R26-YFP* brain and almost no YFP$^+$ cells in *Tmem119*$^{CreER}$ or *P2ry12*$^{CreER}$*R26-YFP* mice (occasionally one YFP$^+$ cell in a whole brain section). Taken together, these data confirm the previously characterized microglia-specific recombination in *Tmem119*$^{CreER}$ and *P2ry12*$^{CreER}$ mice and document low rates of TAM-independent Cre recombination (leakiness) in these lines. Additionally, we observed leakiness in both *Cx3cr1*$^{CreER}$ lines, with the greatest relative leakiness observed in the *Cx3cr1*$^{YFP–CreER(Litt)}$ line.

## Gene targeting efficiency is related both to intrinsic CreER expression/activity and inter-*loxP* target length

Our data above show that the *Tmem119*$^{CreER}$ and *P2ry12*$^{CreER}$ lines are able to achieve highly efficient recombination in the *Ai9* allele (94.55% and 95.81%, respectively), whereas the recombination efficiency in the *R26-YFP* allele is comparatively less (34% and 37%, respectively; Figure 1, bottom). Similarly, the rates of TAM-dependent recombination in the *Cx3cr1*$^{CreER(Jung)}$ line is higher with the *Ai9* versus the *R26-YFP* allele (99% vs. 89%). We considered whether this apparent difference in reporting is due to inter-*loxP* distance (or possibly other differences in reporter gene expression, stability, or fluorescence intensity) and not genomic location or DNA accessibility because both the *Ai9* and the *R26-YFP* reporter gene are inserted into the *R26* locus. We therefore generated *P2ry12*$^{CreER}$*Ai9/R26-YFP* double reporter mice and examined the number and relative intensity of recombined cells on a single-cell basis using flow cytometry and immunohistochemistry (Figure 2). Using FACS analysis, we observe that tdTomato$^+$ cells are more abundant among reporter$^+$ cells (percentage of tdTomato$^+$ cells among all reporter$^+$ cells = 82.52%, YFP$^+$ cells among all reporter$^+$ cells = 41.55%; $p < 0.001$, Student's t test; Figure 2; Table S1). However, there are also YFP$^+$ cells that are negative for the tdTomato reporter (average = 17.48% of the total reporter$^+$ cells; Figure 2). Immunohistochemistry (IHC) confirmed a similar trend in percentage of reporter$^+$ cells, with lower but evident YFP$^+$/tdTomato$^-$ cells (Figure 2). These results suggest that, although the shorter-length floxed *Ai9* reporter allele has a higher probability of recombination on a population level, the recombination of the two different alleles in the same genomic locus is regulated independently; in any single cell, which allele is recombined is independent of the recombination of the alternate allele and does not always follow the size rule, which rather suggests a probabilistic distribution that is related to the *loxP* distance. Similarly, recombination of a single copy of the reporter allele likely

does not always guarantee the recombination of floxed alleles of any given target gene, especially when using a floxed reporter allele that has a short floxed region, such as *Ai9*.

To more directly investigate the efficiency of microglial recombination, we generated different combinations of $Cx3Cr1^{CreER(Jung)}$ (apparent "strong" *Cre*) or $P2ry12^{CreER}$ (apparent "weak" *Cre*) bred to the following floxed alleles with varying inter-*loxP* distances (bred to homozygosity): $Tgfb1^{fl/fl(ex3)}$ (*loxP* distance, <0.5 kb), $Alk5^{fl/fl(ex3)}$ (*loxP* distance, 1.6–1.7 kb). Mice were bred with a recombination reporter (*R26-YFP* or *Ai9*) to facilitate the isolation of microglia cells that have undergone at least one recombination event. Total RNA was extracted from sorted microglia cells in all mouse lines, followed by cDNA library preparation and real-time qPCR using allele-specific forward and reverse primers spanning the floxed and neighboring exon. The absence of gene amplification therefore indicates the deletion of floxed exons. At the beginning of the study, microglia were sorted without the application of transcriptional and translational inhibitors. Our sorting protocol was later modified to include these inhibitors to prevent changes in microglial gene expression during the sorting process.[21] However, to examine whether the enzymatic digestion and sorting protocol used in this study alters *Tgfb1* or *Alk5* expression in microglia, we sorted wild-type microglia in the presence or absence of these inhibitors, and our data support that neither *Tgfb1* nor *Alk5* mRNA levels show a difference with or without inhibitors (Figure S5). Therefore, all data presented are pooled from the earlier samples without inhibitors and the later samples with inhibitors.

It is interesting to note that, although we observed substantial recombination of the tdTomato reporter (easier to recombine) in vehicle-treated mice in the $Cx3cr1^{CreER(Jung)}$ line (Figure 1), we did not observe any significant changes in mRNA levels of the floxed target genes (neither *Tgfb1* nor *Alk5*) in sorted microglia from vehicle-treated $Cx3cr1^{CreER(Jung)}$ $Tgfb1^{fl/fl}$ or $Alk5^{fl/fl}$ mice (Figure S6). In the presence of TAM, our results (Figure 3) show that the $Cx3cr1^{CreER(Jung)}$ line leads to significant and almost complete loss of the floxed exon in total RNA content for both $Cx3cr1^{CreER(Jung)}Tgfb1^{fl/fl}$ and $Cx3cr1^{CreER(Jung)}Alk5^{fl/fl}$ mice (Figure 3; 0.0024% for the *Tgfb1* mRNA level compared with control mice and 3.9% for the *Alk5* mRNA level compared with control mice). *Iba1* mRNA levels in the sorted $YFP^+$ microglia are not altered from the $Cx3cr1^{CreER(Jung)}Tgfb1^{fl/fl}$ mice nor the $Cx3cr1^{CreER(Jung)}Alk5^{fl/fl}$ lines, indicating similar enrichment of sorted microglia and that gene deletion is specific to the targeted floxed allele. Because $Cx3cr1^{CreER(Jung)}$ mice recombine the *R26-YFP* reporter allele in most microglia (89%), this result reflects a highly efficient deletion of the target exons. In contrast, $P2ry12^{CreER}$-mediated recombination resulted in an ~50% reduction in both the *Tgfb1* and *Alk5* floxed gene regions. Because $P2ry12^{CreER}$ only recombines ~30% of all microglia at the *R26-YFP* locus, and our sorting strategy enriches for $YFP^+$ cells, this efficiency rate is likely overestimating true recombination efficiency at the gene of interest in the total microglia population. Indeed, in $P2ry12^{CreER}Alk5^{fl/fl}Ai9$ mice (with the easier-to-recombine *Ai9* reporter), while more than 95% of sorted $IBA1^+$ microglia were $tdTomato^+$, there is only a 16% decrease in *Alk5* mRNA in $tdTomato^+$ microglia compared with the wild-type (WT) control (Figure 3), indicating a lower overall recombination efficiency in $P2ry12^{CreER}$ mice compared with the $Cx3cr1^{CreER(Jung)}$ line. In an effort to increase the recombination efficiency of the $P2ry12^{CreER}$ mouse lines, we generated $P2ry12^{CreER(mut/mut)}Tgfb1^{fl/fl}$ and

*P2ry12*$^{CreER(mut/mut)}$*Alk5*$^{fl/fl}$ mice, which carry homozygous *CreER* alleles. Homozygous *CreER* alleles resulted in a higher recombination efficiency in the deletion of both the floxed *Tgfb1* gene (Figure 3; heterozygous Cre, 50% decrease and homozygous Cre, 90% decrease in total *Tgfb1* mRNA levels) and the floxed *Alk5 gene* (heterozygous Cre, 50% decrease and homozygous Cre, 95% decrease in total *Alk5* mRNA levels) among YFP$^{+}$ reporter-expressing microglia.

Taken together, our data suggest that both intrinsic *CreER* activities and target gene inter-*loxP* distance are important determinants in gene excision. Our results also highlight critical differences in apparent gene targeting efficiency when using various reporters, specific assessment of allele-specific gene loss, or methods to isolate/analyze a conditional gene targeting experiment (e.g., FACS versus IHC).

## Lack of *iSuReCre* allele recombination by *P2ry12CreER* or *Cx3cr1CreER* drivers

As an alternative method to using homozygous *P2ry12*$^{CreER}$ alleles, we were interested in whether we might enhance recombination while maintaining cellular specificity using some of the recently developed tools to further amplify Cre activity. The new *iSuReCre* mouse line, with Cre-inducible expression of both Cre recombinase and the membranous (Mb) Tomato reporter (Figure 4), was made to accomplish this exact goal.[19] The *iSuReCre* construct is designed to induce constitutive Cre expression following transient TAM-induced *CreER* activation with the addition of *P2A-MbTomato* in the *iSuReCre* allele to track constitutive *Cre* induction. We generated *P2ry12*$^{CreER}$*iSuReCre* mice, treated them with TAM at 4–8 weeks of age, then harvested and analyzed brains 2–4 weeks later. Our results (Figures 4A-4H) show that the addition of the *iSuReCre* allele failed to label any microglia with the MbTomato reporter in the *P2ry12*$^{CreER}$ line. Interestingly, there was sparse MbTomato labeling of neurons in the cortex and striatum of *P2ry12*$^{CreER}$*iSuReCre* mice that did not receive TAM (Figures 4A-4H), likely representing ectopic TAM-independent and cre-independent expression of MbTomato from the *iSuReCre* locus because we never observed neuronal recombination in *P2ry12*$^{CreER}$*R26-YFP* or *P2ry12*$^{CreER}$*Ai9* mice. To further test whether the stronger *Cx3cr1*$^{CreER}$ driver could induce *iSuReCre* cassette expression in microglia, we also generated the *Cx3cr1*$^{CreER(Jung)}$*iSuReCre* mice and treated them with TAM. Despite the confirmed recombination efficiency of the *Cx3cr1*$^{CreER}$ line,[18,22] we did not observe any microglia-specific iSuRe reporter MbTomato expression (Figures 4I-4P, ii). To examine whether the iSuRe mouse model works properly in other non-microglia, brain-specific Cre drivers, we generated double cortin *(DCX)*$^{CreER}$*iSuRe-Cre* mice as a positive control (Figure 4, iii). *DCX*$^{CreER}$ mice target immature DCX$^{+}$ neuroblasts in the dentate gyrus, which later develop into mature neuronal nuclei (NEUN)$^{+}$ neurons 4 weeks after administration of TAM. Indeed, brains from *DCX*$^{CreER}$*iSuReCre* mice had strong MbTomato expression in DCX$^{+}$ neuroblasts (Figures 4Q-4T, iii) at 5 days and in mature NEUN$^{+}$/DCX$^{-}$ neurons at 4 weeks (Figures 4U-4X, iii) after TAM administration, respectively. These data confirm that the *iSuReCre* allele is recombined by *DCX*$^{CreER}$, similar to other *Cre* and *CreER* lines tested in the original publication,[19] but our data show that the *iSuReCre* allele is not recombined in adult microglia by multiple driver lines, such as *Cx3cr1*$^{CreER(Jung)}$ or *P2ry12*$^{CreER}$.

## Persistent recombination of splenic macrophages in microglia *CreER* lines

One potential downside of using *Cx3cr1*$^{CreER}$-based strategies in lineage tracking and conditional mutagenesis experiments is these lines' known recombination of circulating blood cells and the potential for these cells to invade and take residence in the CNS. With this in mind, strategies were developed to specifically label brain microglia vs. peripheral monocytes/macrophages, followed by a waiting period of more than 3 weeks after TAM administration to allow the turnover of circulating cells by non-recombined CX3CR1$^{-}$ bone marrow progenitors.[23,24] However, these strategies are cumbersome or not feasible in developmental and injury contexts, where recombination and engraftment occur more rapidly than the 3-week "washout period" and might include cells derived from non-myeloid (non-marrow) sources. The spleen is a particularly important site for the storage and rapid deployment of monocytes in the setting of development and inflammation[25-27] and can be used as a surrogate for circulating monocytes with recombination activity.

To this end, we examined the expression of recombination reporter genes in the spleen (matched to brain recombination; Figure 1) 4 weeks after TAM or vehicle treatment (Figure 5). In *Cx3cr1*$^{YFP\text{-}CreER(Litt)}$*Ai9* mice, we observed substantial TAM-independent base-level tdTomato and YFP reporter expression in IBA1$^{+}$ splenic macrophages and a strong increase in reporter recombination/expression with persistence of these cells 4 weeks after TAM administration, mirroring TAM -independent and -dependent reporter recombination in the brain (Figure 1). We observed non-negligible recombination of splenic macrophages in *P2ry12*$^{CreER}$*Ai9* mice (as reported previously[8] but less recombination of splenic macrophages in *Tmem119*$^{CreER}$ mice (Figures 5H-5M). Interestingly, there was strong recombination of non-myeloid (IBA1$^{-}$) cells, which, by comparison with the brain, may represent splenic adventitial fibroblasts.[28] These data highlight a relatively high degree of recombination in non-microglial splenic macrophages in *Cx3cr1*$^{CreER}$ (TAM-treated and untreated) and *P2ry12*$^{CreER}$ (TAM-treated) mice, representing a reservoir of recombined cells that could replace microglia and complicate the interpretation of lineage tracing and gene deletion experiments using these lines.

## Off-target effects of TAM -induced microglial *CreER* activity

A recent evaluation of the *Cx3cr1*$^{YFP\text{-}CreER(Litt)}$ line found that neonatal TAM exposure resulted in microglia with reduced expression of homeostatic genes and reciprocal induction of activation genes related, in part, to interferon signaling.[14] Notably, *Tmem119*$^{CreER}$ did not show this same Cre-mediated off-target effect in early postnatal microglia, and administration of TAM to adult *Cx3cr1*$^{YFP\text{–}CreER(Litt)}$ mice showed no major phenotype. Given the high efficiency of *Cx3Cr1*$^{CreER}$ mouse lines in targeting microglia on a populational level and likely still popular usage in future microglia gene knockout studies, we looked to determine whether this same phenotype existed in other microglia-targeting *CreER* lines.

*Cx3cr1*$^{YFP\text{-}CreER(Litt)(mut/WT)}$, *Cx3cr1*$^{CreER(Jung)(mut/WT)}$, and *P2ry12*$^{CreER(mut/WT)}$ mice were intercrossed with WT mice, and newborn pups were given TAM on post-natal days 1 (P1), P2, and P3 or P4, P5, and P6, and then brains were harvested and analyzed on P15 or P30 (Figure 6). For convenience, we used brains from mice with either a *Tgfbr2*$^{fl/wt}$

or *Tgfb1*$^{fl/wt(ex1)}$ allele already in our colonies. In neonatally induced *Cx3cr1*$^{YFP\text{-}CreER(Litt)(mut/WT)}$ mice, we observed widespread loss of the homeostatic marker P2RY12 in IBA1$^{+}$ microglia, accompanied by their adoption of a less ramified morphology (Figure 6A). In contrast, and similar to a published report,[14] TAM administration to *Cx3cr1*$^{YFP\text{-}CreER(Litt)(mut/WT)}$ mice after P21 had no apparent effect on microglia homeostasis or activation (Figure 6B). Likewise, we observed no apparent phenotypic changes in neonatally induced *Cx3cr1*$^{YFP\text{-}CreER(Jung)(mut/WT)}$ or *P2ry12*$^{CreER(mut/WT)}$ mice (Figure 6C). These experiments were repeated and confirmed in two different research laboratories (the Luo Lab, University of Cincinnati, and the Arnold Lab, University of California, San Francisco) to control for the possibility that differences in vivarium microbiomes or research technique (e.g., immunoprecipitation [IP] injection-induced peritoneal infection/inflammation), as described recently in cerebral cavernous malformation (CCM) mouse models,[29] might contribute to the observed loss of microglia homeostasis in *Cx3cr1*$^{YFP\text{-}CreER(Litt)}$ mice.

When investigating the microglia phenotype observed in *Cx3cr1*$^{CreER(Litt)}$ mice, by analyzing previously published RNA sequencing (RNA-seq) datasets, we were struck by its similarity to microglia deficient in transforming growth factor β (TGF-β) signaling (*Itgb8*$^{fl/fl}$*;Nestin*$^{Cre}$ and *Tgfbr2*$^{fl/fl}$*;Cx3cr1*$^{CreER}$,[30] *Tgfb1*$^{-/-}$,[31] *Tgfbr2*$^{fl/fl}$*Sall1*$^{CreER}$,[15] and *Lrrc33/Nrro*$^{-/-}$[16]), including loss of homeostatic signature genes such as *P2ry12, HexB, SiglecH*, and *Tmem119* with reciprocal upregulation of MgND/DAM (neurodegeneration-associated phenotype by microglia/disease-associated microglia) signature genes, including *ApoE, Axl*, and *Lgals3*, and genes directly or indirectly related to interferon signaling, including *Irf7, Siglec1*, and *Mx1* (Figure 7A). Indeed, the transcriptional phenotype of microglia from neonatal (P15) *Tgfbr2*$^{fl/fl}$*;Cx3cr1*$^{CreER}$ mice is moderately correlated with that those from neonatal TAM-treated *Cx3cr1*$^{YFP\text{-}CreER(Litt)}$ mice ($R = 0.56$, $p > 2e{-}16$). Importantly, these various TGF-β signaling-deficient mouse models were not generated using the *Cx3cr1*$^{YFP\text{-}CreER(Litt)}$ line, raising the hypothesis that neonatal TAM administration to *Cx3cr1*$^{YFP\text{-}CreER(Litt)}$ mice might somehow dysregulate TGF-β signaling. We directly tested this by immunostaining mouse brains for phosphorylated (p) SMAD3 (suppressor of mothers against decapentaplegic), an indicator of canonical (SMAD-mediated) TGF-β signaling. While there was a trend for reduced pSMAD3 immunofluorescent staining in microglia from TAM-treated compared with non-TAM-treated controls, the overall change at the population level was not significantly different (Figures 7C and 7D). These results suggest that reduced TGF-β signaling is not likely a primary driver of the microglial phenotype in TAM-treated neonatal *Cx3cr1*$^{YFP\text{-}CreER(Litt)}$ mice but could be a downstream consequence of increased interferon (INF) signaling as proposed by Sahasrabuddhe and Ghosh.[14] Consistent with this, INF and TGF-β/SMAD signaling are co-regulated in non-homeostatic microglia,[32] and SMAD2/3 is known to directly regulate the expression of several homeostatic markers, including *P2ry12*.[33]

## DISCUSSION

The use of the Cre-*loxP* system has revolutionized biological research by enabling cell-type-specific gene manipulation. The addition of temporal control to *Cre* activity was introduced by the addition of a modified estrogen receptor (ER) ligand binding domain,[34] providing exquisite precision when targeting and tracking ontogenically distinct cell subtypes and their

associated lineages. The application of Cre-based genetic targeting to microglia biology has had particularly important impacts on our understanding of brain immunity. Over the past decade, research utilizing two *Cx3Cr1*$^{CreER}$ lines[17,18] helped to elucidate the ontogeny of microglia and non-microglia CNS-associated macrophages and the roles of specific microglia genes and signaling pathways in brain development and function.[18,35] Recently, in an effort to improve the specificity of brain microglia gene manipulation, several new brain microglia-specific inducible *CreER* mouse lines were generated, including *Tmem119*$^{CreER}$, *P2ry12*$^{CreER}$ *Sall1*$^{CreER}$, and *HexB*$^{CreER}$.[8-10,15] Since the initial reports characterizing these new lines, we and others noticed different degrees of leakiness and recombination efficiency. Furthermore, recent reports document important off-target effects in *Cx3cr1*$^{YFP\text{-}CreER(Litt)}$ mice,[12,14] prompting us to perform a more detailed characterization of the publicly available microglia-targeting *CreER* lines. Our studies focus on five key characteristics of *CreER* gene targeting: specificity, leakiness, efficiency, extraneural recombination, and off-target effects. Each of these characteristics was examined in both male and female mice, and no major differences were observed. Because *Sall1*$^{CreER}$ and *Hexb*$^{CreER}$ were not readily available to us at the time of this study, we compared our results with published studies using these lines.[9,15] We believe this evaluation will provide valuable information to the field, particularly for researchers aiming to identify appropriate mouse models for conditional gene deletion in microglia. For a summary of our and previous studies, please see Table 1 for findings in adult mice and Table 2 for findings during developmental/neonatal stages.

## Specificity

*Cx3cr1*$^{YFP\text{-}CreER(Litt)}$ and *Cx3cr1*$^{CreER(Jung)}$ recombine microglia and other CNS (brain border) macrophages, myeloid precursors, and dendritic cell subsets in the meninges. *P2ry12*$^{CreER}$ specifically recombines microglia in addition to a small subset of dural and choroid plexus macrophages (likely epiplexus cells). *Tmem119*$^{CreER}$ recombines microglia and non-macrophage meningeal/perivascular cells (likely fibroblasts) and a small subset of choroid plexus macrophages. *HexB*$^{CreER}$ has been shown to provide specific CNS-microglia recombination without labeling neurons, astrocytes, oligodendrocytes, or vascular cells in the brain and can distinguish CNS-associated macrophages (CAMs) from microglia.[9] *Sall1*$^{CreER}$ specifically recombines microglia in addition to neurons, astrocytes, and oligodendrocytes.[15]

## Leakiness

We found that *Cx3cr1*$^{CreER}$ lines (Littman and Jung) recombined the more sensitive *Ai9-tdTomato* reporter in a relatively large number of microglia (and splenic macrophages) in the absence of TAM, whereas *Tmem119*$^{CreER}$ and *P2ry12*$^{CreER}$ lines were comparatively less leaky. *Sall1*$^{CreER}$ is relatively more leaky than *Hexb*$^{CreER}$ and similar to *Cx3cr1*$^{CreER(Jung)}$. These three lines have been compared previously using both *ROSA26-YFP* and *Ai9* reporter mice to assess leakiness.[9] Similar to our findings, this group observed that leakiness was negatively correlated with recombination efficiency and the length of the *loxP* flanked region (higher leakiness in the *Ai9* reporter and lower leakiness in the *R26-YFP* reporter). However, it is interesting to note that, although the *Cx3cr1*$^{CreER(Jung)}$ line shows moderate TAM-independent expression of the *Ai9* reporter, total sorted microglia (CD11b$^{positive}$/CD45$^{low}$) showed no difference in *Tgfb1* or *Alk5* mRNA levels in vehicle-

treated *Cx3cr1*$^{CreER(Jung)}$*Tgfb1*$^{fl/fl}$ or *Cx3cr1*$^{CreER(Jung)}$*Alk5*$^{fl/fl}$ mice. Despite this, it is still recommended for future studies to include no-TAM control groups in addition to non-floxed and TAM controls.

## Efficiency

Efficiency was directly correlated with inter-*loxP* distance and intrinsic *CreER* activity/expression. *Tmem119*$^{CreER}$ and *P2ry12*$^{CreER}$ mice with the *Ai9* reporter (0.9 kb) maintained high recombination efficiency but only achieved partial recombination in the *R26-YFP* reporter (2.7 kb) allele (about 30% of all microglia populations), reiterating the importance of *loxP* distance in recombination efficiency. In line with this conclusion, we found that the *Cx3Cr1*$^{CreER(Jung)}$ line effectively deleted both copies of the shorter *Tgfb1*$^{fl/fl}$ target gene and the longer *Alk5*$^{fl/fl}$ gene, while *P2ry12*$^{CreER}$ had an ~50% decrease in mRNA levels of these two floxed genes. It is worth noting that this 50% gene deletion efficiency in the *P2ry12*$^{CreER}$ line was evaluated in sorted YFP$^{+}$ microglia populations. Because *P2ry12*$^{CreER}$ only achieves *R26-YFP* reporter induction in about 30% of total microglia, the gene deletion efficiency in the full population of microglia sorted using the *Ai9-tdTomato* reporter was even lower (15% decrease in *Alk5* mRNA levels in total tdTomato$^{+}$ cells). Masuda et al.[9] directly compared *HexB*$^{CreER}$, *Sall1*$^{CreER}$, and *Cx3cr1*$^{CreER(Jung)}$ and found *HexB*$^{CreER}$ and *Sall1*$^{CreER}$ to be similarly less efficient than *Cx3cr1*$^{CreER}$. Note that most of their analysis was done using homozygous *Hexb*$^{CreER(mut/mut)}$ mice, which likely increased recombination efficiency, as we observed with *P2ry12*$^{CreER(mut/mut)}$mice (heterozygous Cre, 50% decrease and homozygous Cre, 90% decrease in total *Tgfb1* mRNA levels; heterozygous Cre, 50% decrease and homozygous Cre, 95% decrease in total *Alk5* mRNA levels; Figure 3).
A recent independent study showed that homozygous *Tmem119*$^{CreER(mut/mut)}$ mice also improves the recombination efficiency of target genes (heterozygous *Cre*, 50%; homozygous *Cre*, 67%).[22]

## Extraneural recombination

Outside of the CNS, *Cx3cr1*$^{YFP\text{-}CreER(Litt)}$ and *Cx3cr1*$^{CreER(Jung)}$ lines recombine peripheral blood and peripheral immune cells, including dendritic cell subsets, T cells, natural killer (NK) cells, and tissue macrophages in most organs, including the spleen. *P2ry12*$^{CreER}$ recombines a subset of tissue-resident macrophages, including a population of splenic macrophages. *P2ry12*$^{CreER}$ does not recombine blood cells or platelets.[8] *Tmem119*$^{CreER}$ recombines a small percentage of IBA1$^{+}$ macrophages and certain IBA1$^{-}$ cells in the spleen (the exact cell types of these tdTomato$^{+}$ cells are not clear). In comparison, *Sall1*$^{CreER}$ does not recombine blood cells, while *HexB*$^{CreER}$ mice have significant acute recombination in LY6C$^{hi}$ and LY6C$^{lo}$ cells (similar to the *Cx3cr1*$^{CreER(Jung)}$ line) and additionally recombine nearly all circulating LY6G$^{+}$ granulocytes.[9] Recombination of blood cells by *Hexb*$^{CreER}$ is paralleled by tdTomato expression in most F4/80$^{+}$/IBA1$^{+}$ splenic myeloid cells[9] from *Hexb*$^{tdt/tdt}$ reporter mice.

## Off-target effects

Our study explored a phenomenon described by Sahasrabuddhe and Ghosh.[14] This group reported that neonatal TAM administration to the *Cx3cr1*$^{YFP\text{-}CreER(Litt)}$ line resulted in induction of microglial IFN-1 signaling, hypothesized to be due to Cre-mediated DNA

damage, and an altered microglia transcriptional profile. They also report that this effect was not observed in TAM -treated adult *Cx3cr1*$^{YFP–CreER(Litt)}$ mice or in *Tmem119*$^{CreER}$ mice with neonatal TAM administration. Interestingly, the transcriptional phenotype of microglia from neonatally induced *Cx3cr1*$^{YFP-CreER(Litt)}$ is similar to *Sall1*$^{fx}$/*Sall1*$^{CreER}$, *Sall1*$^{fl/fl}$;*Cx3cr1*$^{CreER(Jung)}$, and *Tgfbr2*$^{fl/fl}$;*Cx3cr1*$^{CreER(Jung)}$ with increased expression of INF response genes and other DAM/MgND genes and downregulation of major homeostatic microglia genes, including *P2ry12, Tmem119, HexB*, and *Sall1* itself. This similarity prompted us to explore whether TGF-β/Smad signaling might be directly affected by neonatal TAM induction in *Cx3cr1*$^{YFP-CreER(Litt)}$, or other microglia-targeting *Cre* lines. We found that, despite robust activation and loss of P2RY12 expression in microglia in *Cx3cr1*$^{YFP-CreER(Litt)}$ mice, pSMAD3 immunofluorescence intensity (a measure of TGF-β signaling) was not appreciably changed. Furthermore, we observed no evidence of alterations in microglia homeostatic gene expression in *Cx3cr1*$^{CreER(Jung)}$ and *P2ry12*$^{CreER}$ lines.

We and others previously investigated whether the gene knockin strategies used to generate these various *CreER* lines might affect gene expression, resulting in unintended effects. *Cx3cr1*$^{YFP-CreER(Litt)}$, *Cx3cr1*$^{CreER(Jung)}$, and *Sall1*$^{CreER}$ lines were generated using a knockin/knockout strategy and so, by definition, have reduced expression of *Cx3cr1* and *Sall1*, respectively. Both genes are known to have important functions in brain development. *Tmem119*$^{CreER}$, *P2ry12*$^{CreER}$, and *Hexb*$^{CreER}$ lines were generated using CRISPR-facilitated homologous recombination in which the target gene stop codon was replaced by a ribosome-skipping fusion peptide coding sequence, followed by the coding sequence for *CreER*. All lines show some diminution in mRNA expression of target gene expression. No brain-specific functions have been found for *Tmem119*. P2RY12 signaling is responsible for inflammation-induced microglia process extension[36] and microglia containment of leakage following cerebrovascular injury.[37] Homozygous loss of *Hexb* in mice causes a fatal demyelinating microgliopathy, similar to *Hexb*-inactivating mutations in patients with Sandhoff's lysosomal storage disease. Considering the known roles of *Cx3cr1, Sall1, P2ry12*, and *Hexb* in development and disease, it is at least theoretically possible that reduction of their gene expression could have unintended experimental effects.

## Additional considerations and recommendations

While the *Cx3Cr1*$^{YFP–CreER(Litt)}$ and *Cx3Cr1*$^{CreER(Jung)}$ lines have been used widely in the field, alternative microglia *CreER* lines are still new to the field. This research highlights the value of a systematic comparison and evaluation of genetic tools to better design experimental strategies for microglia conditional gene manipulation. While we tried to be thorough in our assessment of the current commercially available tools, there are still several microglia-specific lines that we did not investigate, including *Sall1*$^{CreER}$ and *Hexb*$^{CreER}$ and a new *Fcrls-2A-Cre* available through JAX (036591). Based on our results, we are able to make the following recommendations regarding choice of *CreER* line and specific experimental goals.

If the key question being investigated requires deletion in all microglia, the two *Cx3cr1*$^{CreER}$ lines are advantageous due to their high recombination efficiency. Comparing the two

*Cx3Cr1*$^{CreER}$ lines (Littman and Jung), our data suggest that the *Cx3*$^{CreER(Jung)}$ line has less Cre activity in the absence of TAM (with both the *Ai9* and *R26-YFP* reporter) while having almost equally high recombination efficiency after TAM treatment. The fused *IRES-EYFP* reporter in *Cx3Cr1*$^{YFP\text{-}CreER(Litt)}$ is convenient for sorting microglia without the need for surface antibody staining, such as CD11b and CD45. However, crossing the *Cx3Cr1*$^{CreER(Jung)}$ line with the *Ai9-tdTomato* or *R26-YFP* reporter line can be easily accomplished to facilitate genetic reporter-based FACS. Because peripheral macrophages also express *Cx3Cr1* and are therefore recombined by *Cx3cr1*$^{CreER}$, peripheral immune effects are a potential confound that needs to be considered when using these two lines.

To investigate gene function specifically in microglia, *Tmem119*$^{CreER}$ and *P2ry12*$^{CreER}$ are preferable. Additional care should be taken with *Hexb*$^{CreER}$, which was found to strongly recombine blood cells.[9] The *Tmem119*$^{CreER}$ or *P2ny12*$^{CreER}$ lines therefore enable enriched labeling of CNS parenchyma microglia and allow researchers to track endogenous microglia and study their specific properties after CNS injury or in neurodegenerative conditions. This was successfully achieved in an experimental autoimmune encephalomyelitis (EAE) model using the *P2ry12*$^{CreER}$ line.[8] Future use of these tools could facilitate the pre-labeling of brain microglia cells and allow the separation of microglia from infiltrating peripheral monocytes/macrophages by FACS. This will help resolve a long-standing question in the field: whether the infiltrating monocytes/macrophages have a distinct neuroinflammatory program compared with the resident brain microglia in CNS disease or injury. The lower recombination efficiency observed in *P2ry12*$^{CreER}$ and *Tmem119*$^{CreER}$ mice (especially in the heterozygous *CreER* mice) also lends itself well to performing mosaic genetic experiments and *in vivo* single-cell phenotypic analyses, where differences among single cells can be attributed to induced gene mutation or expression in an otherwise identical organism and genetic background.

We attempted to enhance recombination efficiency of the *P2ry12*$^{CreER}$ line by crossing to the *iSuReCre* reporter mouse. Compared with *DCX*$^{CreER}$*;iSuReCre* mice, with robust recombination of immature DCX$^{+}$ neuroblasts, we observed no microglial recombination in *P2ry12CreER;iSuReCre* mice based on immunostaining brain sections for the *iSuReCre* MbTomato reporter. Interestingly, *iSuReCre* shows reliable recombination and tdTomato expression in peripheral macrophages by *LysMCre*, and *Tie2Cre;iSuReCre* mice have apparently strong recombination of retinal microglia. The underlying cause for lack of *iSuReCre* recombination by *P2ry12*$^{CreER}$ mice is unknown but may be due to the genomic integration site of the *iSuReCre-tdT* construct, which has not been as well characterized as the *ROSA26* safe harbor locus. Our data for the *Cx3cr1*$^{CreER(Jung)}$ *iSureCre* mice show that, even with the strong *Cx3cr1*$^{CreER}$ driver, MbTomato expression is absent in microglia, supporting the hypothesis that the specific loci where the *iSuRe-Cre* cassette is inserted might be silenced in microglia. An alternative method to boost *CreER* activity is to breed the line to homozygosity. Indeed, *P2ry12*$^{CreER/CreER}$ (Figure 3) and *Hexb*$^{CreER/CreER}$ mice[22] have more efficient gene deletion. Additionally, an investigator can choose to breed in one knockout allele to reduce the number of recombination events required for complete gene deletion.

When using the *Tmem119*$^{CreER}$ or the *P2ry12*$^{CreER}$ lines, we recommend using a reporter with inter-*loxP* distance as close to that of the target gene as possible, to include one knockout allele so that only one recombination event is required for gene deletion (if heterozygous knockout mice do not cause phenotype), or ideally to utilize one target allele that is floxed with an intrinsic reporter (knockin/knockout construct) and one knockout allele to simultaneously facilitate gene deletion and precisely identify knockout cells. Understanding that null and conditional knockout-knockout reporters and other Cre "boosting" constructs are not readily available, additional analysis, such as real-time qPCR on sorted microglia, RNAscope, or IHC staining, is recommended to validate successful knockout or knockdown of the target genes in brain microglia. We recommend performing this validation in a small pilot study before investing time and resources in larger-scale experiments.

With our rigorous and careful analysis of the four commercially available microglia-*CreER* mouse lines, focusing on the five key features we chose, we identify important caveats and strengths for these lines, which will be of broad significance for researchers interested in performing conditional gene deletion in microglia. While we were preparing this manuscript, a preprint of an independent study evaluating microglial *CreER* lines was reported,[22] including evaluation of *HexB*$^{CreER}$ mice. Our two studies provide both overlapping and distinct recommendations and guidelines for the use of these powerful tools. Together with this study, we hope our rigorous comparison and analysis provides important data and guidance for researchers interested in performing conditional gene manipulation in microglia.

## Limitations of the study

While the data we reported in this study characterize several key characteristics of current commercially available microglial *CreER* lines, we aim to be transparent with the limitations of our study to aid future experimental design. Our study did not elucidate the mechanism that determines recombination efficiency. An excellent way to test this mechanism in the future could be to examine the CRE protein level in each of the lines. While we did not pursue this approach, based on our comparison of the *P2ry12*$^{CreER}$ heterozygous and homozygous mice for recombination efficiency, it appears that the amount of CRE expression can be increased to improve the recombination efficiency of floxed target genes.

We also provided data showing persistent Cre-reporter expression in the spleen of the animals in certain *CreER* mouse lines. While this suggests remaining Cre-recombined cells in the spleen at 4 weeks after TAM treatment, we did not verify Cre-mediated deletion in the spleen with our floxed target genes (such as *Tgfb1*$^{fl/fl}$ or *Alk5*$^{fl/fl}$ mice). Also, we did not examine recombination in other peripheral organs. Examining recombination in other peripheral organs is essential if experimental investigations could be influenced by peripheral gene modification or peripheral reporter expression.

The TAM dosage regimen used in our study (180 mg/kg for 5 consecutive days) is relatively high compared with the dosage regimen used by other studies. We and others have used this dosage of TAM in previous studies with minimal effect on the survival or general health of mice.[38-42] While TAM has been reported to have adverse effects on certain cell types,[43-45]

we did not observe any morphological or homeostatic signature gene changes in microglia due to the administration of TAM compared with vehicle controls while achieving consistent and efficient recombination in the *Cx3cr1*$^{CreER}$ lines. It is important to note that, even with this high dosage of TAM, the *Tmem119*$^{CreER}$ and *P2ry12*$^{CreER}$ lines showed substantially lower recombination efficiency compared with the *Cx3cr1*$^{CreER}$ lines, especially in the heterozygous *CreER* mice.

Additional limitations of our study include the fact that, while we used both male and female mice and did not observe any apparent sex-dependent differences in any of the features we evaluated, we did not analyze sex as a biological variable. In experiments related to Figure 6C, we analyzed microglial homeostasis in neonatally induced *Cx3cr1*$^{YFP\text{-}CreER(Litt)}$, *Cx3cr1*$^{CreER(Jung)}$, and *P2ry12*$^{CreER}$ mice. *Cx3cr1*$^{CreER(Jung)}$ and *P2ry12*$^{CreER}$ lines also had one floxed allele of either *Tgfbr2* or *Tgfb1* because these mice were readily available in our colony. As shown in Figure 7, the loss of TGF-β signaling itself leads to loss of microglial homeostasis. Therefore, the absence of this phenotype in heterozygous *(*$^{fl/WT}$*) CreER* mice suggests that there is no loss of microglial homeostasis in these heterozygous mice in the presence of *Cx3cr1*$^{CreER(Jung)}$ and the *P2ry12*$^{CreER}$ driver.

# STAR★METHODS

## RESOURCE AVAILABILITY

**Lead contact—**Further information and requests for resources and reagents should be directed to and will be fulfilled by the Lead Contact, Yu Luo (luoy2@ucmail.uc.edu).

**Materials availability—**This study did not generate new unique reagents.

### Data and code availability

1. We analyzed recently published publicly available RNA-seq datasets: GEO: GSE190207 and GEO: GSE124868.
2. Microscopy data and behavioral test data reported in this paper will be shared by the lead contact upon request.
3. No original code was generated in this study.
4. Any additional information required to reanalyze the data reported in this paper is available from the lead contact upon request.

## EXPERIMENTAL MODEL AND STUDY PARTICIPANT DETAILS

**Animals—**All animal protocols were approved by the IACUC of University of Cincinnati or the IACUC of University of California, San Francisco. All transgenic lines (see details below) and C57BL/6J WT mice were purchased from Jackson Laboratory and housed in the animal facility of the University of Cincinnati or University of California, San Francisco. Mice were maintained with a 12-h light/dark cycle and fed *ad libitum*. To evaluate Cre recombinase specificity and efficiency, we utilized four different microglia CreER lines: *Cx3cr1-*$^{YFP\text{-}CreER(Litt)}$ Line (JAX stock number 021160)[17]; *Cx3cr1*$^{CreER(Jung)}$ Line (JAX stock number 020940)[18]; *Tmem119*$^{CreER}$ line (JAX stock number 031820)[10]

and the *P2ry12*$^{CreER}$ line (JAX stock number 034727).[8] For fluorescent reporter lines, we crossed the above microglia CreER lines with either the *Ai9 R26-CAG-tdTomato* line (JAX stock number 007909)[46] or the *ROSA26-YFP* line (JAX stock number 006148)[47] or both of the reporter lines in some of the experiments. To analyze target gene deletion efficiency with the different floxed l between the two *loxP* sites, we generated *Cx3cr1*$^{CreER(Jung)}$ or *P2ry12*$^{CreER}$-*Tgfb1*$^{fl/fl}$ mice (floxed exon 3, ~500 bp, JAX stock number 65809) or *Cx3cr1*$^{CreER(Jung)}$ or *P2ry12*$^{CreER}$-*Alk5*$^{fl/fl}$ mice (Floxed region is between 1.6 and 1.7 kb, JAX stock number 028701).[48] To investigate whether the iSuRe-Cre transgene is inducible in microglia in the *P2ry12*$^{CreER}$ line and the *DCX*$^{CreER}$ line,[49] *iSuRe-Cre*[19] mouse line is obtained from Dr. Rui Benetido (Centro Nacional de Investigaciones Cardiovasculares -CNIC, Spain) and crossed with the *P2ry12*$^{CreER}$, *Cx3cr1*$^{CreER(Jung)}$ or *DCX*$^{CreER}$ mouse line to generate *P2ry12*$^{CreER(mut/WT)}$*iSuRe-Cre*$^{(mut/WT)}$, *Cx3cr1*$^{CreER(Jung)(mut/WT)}$iSuRe-Cre$^{(mut/WT)}$ or *DCX*$^{CreER(mut/WT)}$iSuRe-*Cre* $^{(mut/WT)}$ mice. Mice of both sexes were used and were bred on a C57BL/6 background. No animals were excluded from data analysis except where tissue preservation quality was not ideal due to unsuccessful perfusion (indicated by shredded tissue) or poor cryoprotection in tissues.

**Tamoxifen treatment *in vivo*—**The variety of MG$^{CreER}$*Ai9* or MG$^{CreER}$*R26YFP* or *P2ry12*$^{CreER}$*Ai9/R26YFP* double reporter mice and the *Tgfb1* and *Alk5* floxed mice (8–12 weeks old, both male and females) were given tamoxifen (TAM) dissolved in 10% EtOH/90% sunflower oil or vehicle without TAM by gavage feeding at a dose of 180 mg/kg daily for 5 consecutive days, administration varied between batches ranging from early morning (8-11a.m.) to later afternoon (2-6p.m.) but no significant difference in recombination efficiency between time points were observed. This dosing regimen was previously demonstrated to provide maximal recombination with minimal mortality and successfully monitored the adult NSCs in previous studies by our group and the others.[40,50] To evaluate recombination efficiency in the brain and the clearance of splenic monocytes/macrophages, we collected the brain and the spleen of VEH or TAM treated mice at 4 weeks after the treatment for immunohistochemical (IHC) or flow cytometry (FACS) analysis. For studying the phenotype of non-homeostatic microglia in *CreER*$^{(mut/WT)}$ mice with TAM treatment, *Cx3cr1*$^{YFP–CreER(Litt)(mut/WT)}$ neonatal mice were subjected to either VEH or TAM treatment at neonatal days of P1-P4 (50μg via intragastric injection) and brain harvested for analysis at p15. To test effect of TAM treatment in the *Cx3cr1*$^{YFP–CreER(Litt)(mut/WT)}$ adolescent mice, mice at 3 weeks of age were treated with 5 day gavage (180 mg/kg daily) and harvested at 4 weeks after TAM treatment. Neonatal *Cx3cr1*$^{CreER(Jung)}$ allele carrying mice (*Cx3cr1*$^{YFP–CreER(Litt)(mut/WT)}$*Tgfbr2*$^{fl/WT}$ *or Tgfb1*$^{WT/fl}$) or *P2ry12*$^{CreER}$ allele carrying mice (*P2ry12*$^{CreER(mut/WT)}$*Tgfb1*$^{fl/WT}$) were subjected to TAM treatment at neonatal days of P1-P4 (50μg via intragastric injection) and brain harvested for analysis at P15 or at neonatal days P4-P6 (500ug via intraperitoneal injection) and harvested at P30.

## METHOD DETAILS

**Immunohistochemistry—**Mice were anesthetized and perfused with PBS or PBS followed by 4% paraformaldehyde (PFA). Mice were perfused and samples were collected from variable time points throughout the day for separate batches, although no observable difference was seen in samples from collected from different time of day. For brains that

were subjected to both IHC and FACS analysis, mice were only perfused with PBS and part of the brain block was drop fixed in 4% PFA overnight before being transferred to 20% then 30% sucrose. For mice that were perfused by 4% PFA, the brain and spleen was dissected and post-fixed in 4% PFA overnight at 4°C and equilibrated in 20% then 30% sucrose. 30 μm-thick sections were cut in a Leica Cryostat and blocked in 4% BSA/0.3% Triton X-100 for 1 h. After blocking, sections were incubated with primary antibodies for 18 h–42 h at 4°C and followed by appropriate secondary antibodies conjugated with Alexa fluorescence 488, 555, 647 or 790. The following primary antibodies were used in this study: IBA1 (Rabbit 1:1000 Wako), P2RY12 (Rabbit 1:200 Anaspec), P2RY12 (Rat 1:500 BioLegend), GFP (Rabbit 1:1000 Invitrogen), PSMAD3 (Rabbit 1:100 Abcam), NEUN (Mouse 1:1000 BioLegend), DCX (Rabbit 1:1000 Cell Signaling). Omission of primary or secondary antibodies resulted in no staining and served as negative controls. Images were acquired by a motorized stage-equipped Leica DM5000B microscope (Leica Microsystems, Bannockburn, IL) equipped with Stereo Investigator image software (MBF Bioscience, Williston, VT) for unbiased sampling of the tissue field. Confocal imaging was carried out on a Leica Stellaris 8 confocal microscope (Leica Microsystems, Bannockburn, IL). Random imaging field was selected by SI with outlined ROI and grid and images were taken at 20× or 40× objectives. Quantification of the percentage of reporter positive cells (tdTomato+ or YFP+) among IBA1+ microglia (in the brain) or macrophage (in the spleen) was carried out by as described in our previous publication[38] using Nikon Element or ImageJ software. At least 3 sections containing the region of interest at similar coronal locations were quantified for each mouse and averaged values (total or average) for each animal were considered as one data point for statistical analysis. Group and treatment information were all blinded to the image analyzer.

**FACS—**Fluorescent activated cell sorting (FACS) was accomplished using a papain dissociation system (9001-73-4, Worthington Biochemical Corporation). To collect tissue, animals were perfused with cold 1x HBSS for 2–3 min. Samples from separate batches were collected at different time of day, but at least one control and one experimental condition were collected per batch. No observable difference was seen between these separate timed collections for the genes we evaluated. The brain was then extracted and mechanically dissociated with a scalpel before using the papain dissociation kit. At the beginning of the study microglia were sorted without the application of transcriptional and translational inhibitors. Our sorting protocol was later modified to include these inhibitors to prevent changes of microglial gene expression during the sorting process. However, our data show that neither *Tgfbl* nor *Alk5* mRNA levels show a difference with or without inhibitors (Figure S5). Therefore, all data presented are pooled from the samples with or without inhibitors. Transcriptional and translational inhibitors actinomycin, anisomycin, and typtolide were used during the tissue homogenization and the enzymatic dissociation steps to prevent dysregulation of microglia states as previously described in Marsh et al.[21] Once dissociated, to remove excess myelin and debris cells were suspended in a 37% percoll solution and spun at 800g for 20 min. The cells were then resuspended in FACS buffer (0.5% BSA in PBS) for sorting. Gating was determined using the tdTomato or yellow fluorescent protein reporter (YFP) expressed by microglia cre line compared to cells isolated from WT control mice for microglia collection on a BD/FACSAria II (BD Biosciences,

Franklin Lakes, NJ). For analysis of targeted floxed allele expression (*Tgfb1*$^{fl/fl}$ or *Alk5*$^{fl/fl}$) in a variety of microglia-specific CreER lines, we sorted YFP$^{+}$ or tdTomato$^{+}$ cells at 3–4 weeks after TAM administration and processed the sorted microglia cells for qRT-PCR for gene expression analysis as described in details below.

**qRT-PCR analysis to evaluate reduction of mRNA levels of the floxed gene alleles (Tgfb1 and Alk5)—**RNA expression levels for housekeeping genes (Hmbs, PGK1), Iba1 and targeted floxed genes (*Tgfb1*$^{fl/fl}$ or *Alk5*$^{fl/fl}$) were determined by Reverse-Transcribed quantitative real-time PCR. RNA was extracted from FACS sorted YFP$^{+}$ or tdTomato$^{+}$ cells using a RNAqueous-Micro Total RNA isolation kit (AM1931, ThermoFisher Scientific). Total RNA was treated with RNase free DNase and cDNA was then generated using iScript cDNA synthesis kit (1708890, BioRad). cDNA levels for Hmbs (hydroxymethylbilane synthase), pGK1 (phosphoglycerate kinase 1) and various target genes were determined, using specific primer/probe sets by quantitative RT-PCR using a Roche Light Cycler II 480 (Roche, Basel, Switzerland). Relative expression level was calculated using the delta Ct method compared to Hmbs as a reference gene and expressed as fold change compared to the average of WT cells for each individual gene. Primers and carboxyfluorescein (FAM) labeled probes used in the quantitative RT-PCR for each gene are listed in the oligonucleotide section. To selectively detect the presence of the floxed region in the *Tgfb1*$^{fl/fl}$ or the *Alk5*$^{fl/fl}$ microglia, the probe based qRT-PCR reactions were selected so that the forward and reverse primers span the exon junctions of the floxed exon and a neighboring exon therefore ensuring the loss of amplification in the case of a successful cre-lox mediated recombination.

**Bioinformatics analysis and quantification of pSMAD3 immunoreactivity in microglia—**We reanalyzed datasets from GSE190207 (*Cx3cr1*$^{YFP–CreER}$ Littman) and GSE124868 (*Tgbfr2 fl/fl;Cx3cr1*$^{Cre}$ at P15). Fastq files were aligned to the mouse genome (mm10) with Rsubread 2.10 and quantified using FeatureCounts. Differential expression analysis was performed with DESeq2 1.36. Heatmaps were made with the pheatmap 1.0 package, while scatterplots were made with ggplot2 and ggrepel.

Quantification of pSMAD3 immunofluorescent staining was determined as previously published[30] using stained cryosections from four neonatal TAM-treated *Cx3cr1*$^{YFP–CreER(Litt)}$ and three vehicle controls at P15. Three randomly chosen confocal images from each sample were taken using the same confocal settings. ImageJ software was used to quantify the number of microglia cell nuclei (DAPI-positive, Iba1-positive), and the intensity of pSMAD3 staining in each microglia cell.

## QUANTIFICATION AND STATISTICAL ANALYSIS

All studies were analyzed using SigmaPlot. Results are expressed by mean ± SEM of the indicated number of experiments. Statistical analysis was performed using the Student’s t test, and one- or two-way analysis of variance (ANOVA), as appropriate, with Tukey post hoc tests. A p value equal to or less than 0.05 was considered significant.

## Supplementary Material

Refer to Web version on PubMed Central for supplementary material.

## ACKNOWLEDGMENTS

Y.L. is supported by NIH grants (R01NS125074, R01AG083164, R01NS107365, and R21NS127177). A.B. is supported by NIH 1F31NS125930-01. K.W. is supported by NIH 1F31NS129204-01A1. T.D.A. is supported by NIH grants (1R01NS119615-01 and R01NS123168). N.S. is supported by institutional funds. We thank Chet Closson and the University of Cincinnati live imaging core (supported by NIH S10OD030402) for technical support. We would like to thank Dr. Rui Benedito for sharing the *iSuReCre* mouse line and Dr. Dr. Zhi-qi Xiong for sharing the $DCX^{CreER}$ mouse line.

## REFERENCES

1. Carroll JA, Race B, Williams K, Striebel JF, and Chesebro B (2021). Innate immune responses after stimulation with Toll-like receptor agonists in ex vivo microglial cultures and an in vivo model using mice with reduced microglia. J. Neuroinflammation 18, 194. [PubMed: 34488805]
2. Nimmerjahn A, Kirchhoff F, and Helmchen F (2005). Resting microglial cells are highly dynamic surveillants of brain parenchyma in vivo. Science 308, 1314–1318. [PubMed: 15831717]
3. Paolicelli RC, Bolasco G, Pagani F, Maggi L, Scianni M, Panzanelli P, Giustetto M, Ferreira TA, Guiducci E, Dumas L, et al. (2011). Synaptic pruning by microglia is necessary for normal brain development. Science 333, 1456–1458. [PubMed: 21778362]
4. Schafer DP, Lehrman EK, and Stevens B (2013). The 'Quad-partite' Synapse: Microglia-synapse interactions in the developing and mature CNS. Glia 61, 24–36. [PubMed: 22829357]
5. Crain JM, Nikodemova M, and Watters JJ (2015). Microglia express distinct M1 and M2 phenotypic markers in the postnatal and adult CNS in male and female mice. J. Neuroscience 91, 1143–1151.
6. Pozzo ED, Tremolanti C, Costa B, Giacomelli C, Milenkovic VM, Bader S, Wetzel CH, Rupprecht R, Taliani S, Settimo FD, and Martini C (2019). Microglial pro-inflammatory and anti-inflammatory phenotypes are modulated by translocator protein activation. Int. J. Mol. Sci 20. 4467–21. [PubMed: 31510070]
7. Kim J-S, Kolesnikov M, Peled-Hajaj S, Scheyltjens I, Xia Y, Trzebanski S, Haimon Z, Shemer A, Lubart A, Van Hove H, et al. (2021). A Binary Cre Transgenic Approach Dissects Microglia and CNS Border-Associated Macrophages. Immunity 54, 176–190.e7. [PubMed: 33333014]
8. McKinsey GL, Lizama CO, Keown-Lang AE, Niu A, Santander N, Larpthaveesarp A, Chee E, Gonzalez FF, and Arnold TD (2020). A new genetic strategy for targeting microglia in development and disease. Elife 9, e54590. [PubMed: 32573436]
9. Masuda T, Amann L, Sankowski R, Staszewski O, Lenz M, Errico PD, Snaidero N, Costa Jordão MJ, Böttcher C, Kierdorf K, et al. (2020). Novel Hexb-based tools for studying microglia in the CNS. Nat. Immunol 21, 802–815. [PubMed: 32541832]
10. Kaiser T, and Feng G (2019). Tmem119-EGFP and Tmem119-CreERT2 Transgenic Mice for Labeling and Manipulating Microglia. eNeuro 6, 0448–518. ENEURO.
11. Wieghofer P, Knobeloch K-P, and Prinz M (2015). Genetic targeting of microglia: Genetic Targeting of Microglia. Glia 63, 1–22. [PubMed: 25132502]
12. Chappell-Maor L, Kolesnikov M, Kim JS, Shemer A, Haimon Z, Grozovski J, Boura-Halfon S, Masuda T, Prinz M, and Jung S (2020). Comparative analysis of CreER transgenic mice for the study of brain macrophages: A case study. Eur. J. Immunol 50, 353–362. [PubMed: 31762013]
13. Van Hove H, Antunes ARP, De Vlaminck K, Scheyltjens I, Van Ginderachter JA, and Movahedi K (2020). Identifying the variables that drive tamoxifen-independent CreERT2 recombination:Implications for microglial fate mapping and gene deletions. Eur. J. Immunol 50, 459–463. [PubMed: 31785096]
14. Sahasrabuddhe V, and Ghosh HS (2022). Cx3Cr1-Cre induction leads to microglial activation and IFN-1 signaling caused by DNA damage in early postnatal brain. Cell Rep. 38, 110252. [PubMed: 35045285]

15. Buttgereit A, Lelios I, Yu X, Vrohlings M, Krakoski NR, Gautier EL, Nishinakamura R, Becher B, and Greter M (2016). Sall1 is a transcriptional regulator defining microglia identity and function. Nat. Immunol 17, 1397–1406. [PubMed: 27776109]

16. Wong K, Noubade R, Manzanillo P, Ota N, Foreman O, Hackney JA, Friedman BA, Pappu R, Scearce-Levie K, and Ouyang W (2017). Mice deficient in NRROS show abnormal microglial development and neurological disorders. Nat. Immunol 18, 633–641. [PubMed: 28459434]

17. Parkhurst CN, Yang G, Ninan I, Savas JN, Yates JR 3rd, Lafaille JJ, Hempstead BL, Littman DR, and Gan WB (2013). Microglia Promote Learning-Dependent Synapse Formation through Brain-Derived Neurotrophic Factor. Cell 155, 1596–1609. [PubMed: 24360280]

18. Yona S, Kim KW, Wolf Y, Mildner A, Varol D, Breker M, Strauss-Ayali D, Viukov S, Guilliams M, Misharin A, et al. (2013). Fate Mapping Reveals Origins and Dynamics of Monocytes and Tissue Macrophages under Homeostasis. Immunity 38, 79–91. [PubMed: 23273845]

19. Fernández-Chacón M, Casquero-García V, Luo W, Francesca Lunella F, Ferreira Rocha S, Del Olmo-Cabrera S, and Benedito R (2019). iSuRe-Cre is a genetic tool to reliably induce and report Cre-dependent genetic modifications. Nat. Commun 10, 2262. [PubMed: 31118412]

20. Fonseca MI, Chu SH, Hernandez MX, Fang MJ, Modarresi L, Selvan P, MacGregor GR, and Tenner AJ (2017). Cell-specific deletion of C1qa identifies microglia as the dominant source of C1q in mouse brain. J. Neuroinflammation 14, 48. [PubMed: 28264694]

21. Marsh SE, Walker AJ, Kamath T, Dissing-Olesen L, Hammond TR, deSoysa TY, Young AMH, Murphy S, Abdulraouf A, Nadaf N, et al. (2022). Dissection of artifactual and confounding glial signatures by single-cell sequencing of mouse and human brain. Nat. Neurosci 25, 306–316. [PubMed: 35260865]

22. Faust TE, Feinberg PA, O'Connor C, Kawaguchi R, Chan A, Strasburger H, Masuda T, Amann L, Knobeloch KP, Prinz M, et al. A comparative analysis of microglial inducible cre lines.

23. Fogg DK, Sibon C, Miled C, Jung S, Aucouturier P, Littman DR, Cumano A, and Geissmann F (2006). A Clonogenic Bone Marrow Progenitor Specific for Macrophages and Dendritic Cells. Science 311, 83–87. [PubMed: 16322423]

24. Ajami B, Bennett JL, Krieger C, Tetzlaff W, and Rossi FMV (2007). Local self-renewal can sustain CNS microglia maintenance and function throughout adult life. Nat. Neurosci 10, 1538–1543. [PubMed: 18026097]

25. Swirski FK, Nahrendorf M, Etzrodt M, Wildgruber M, Cortez-Retamozo V, Panizzi P, Figueiredo JL, Kohler RH, Chudnovskiy A, Waterman P, et al. (2009). Identification of Splenic Reservoir Monocytes and Their Deployment to Inflammatory Sites. Science 325, 612–616. [PubMed: 19644120]

26. Bao Y, Kim E, Bhosle S, Mehta H, and Cho S (2010). A role for spleen monocytes in post-ischemic brain inflammation and injury. J. Neuroinflammation 7, 92. [PubMed: 21159187]

27. Chen H-R, Sun YY, Chen CW, Kuo YM, Kuan IS, Tiger Li ZR, Short-Miller JC, Smucker MR, and Kuan CY (2020). Fate mapping via CCR2-CreER mice reveals monocyte-to-microglia transition in development and neonatal stroke. Sci. Adv 6, eabb2119. [PubMed: 32923636]

28. Pezoldt J, Wiechers C, Erhard F, Rand U, Bulat T, Beckstette M, Brendolan A, Huehn J, Kalinke U, Mueller M, et al. (2021). Single-cell transcriptional profiling of splenic fibroblasts reveals subset-specific innate immune signatures in homeostasis and during viral infection. Commun. Biol 4, 1355. [PubMed: 34857864]

29. Tang AT, Choi JP, Kotzin JJ, Yang Y, Hong CC, Hobson N, Girard R, Zeineddine HA, Lightle R, Moore T, et al. (2017). Endothelial TLR4 and the microbiome drive cerebral cavernous malformations. Nature 545, 305–310. [PubMed: 28489816]

30. Arnold TD, Lizama CO, Cautivo KM, Santander N, Lin L, Qiu H, Huang EJ, Liu C, Mukouyama YS, Reichardt LF, et al. (2019). Impaired αVβ8 and TGFβ signaling lead to microglial dysmaturation and neuromotor dysfunction. JJ. Exp. Med 216, 900–915.

31. Butovsky O, Jedrychowski MP, Moore CS, Cialic R, Lanser AJ, Gabriely G, Koeglsperger T, Dake B, Wu PM, Doykan CE, et al. (2014). Identification of a unique TGF-β–dependent molecular and functional signature in microglia. Nat. Neurosci 17, 131–143. [PubMed: 24316888]

32. Cohen M, Matcovitch O, David E, Barnett-Itzhaki Z, Keren-Shaul H, Blecher-Gonen R, Jaitin DA, Sica A, Amit I, and Schwartz M (2014). Chronic exposure to TGF β1 regulates myeloid

cell inflammatory response in an IRF 7-dependent manner. EMBO J. 33, 2906–2921. [PubMed: 25385836]

33. Gosselin D (2020). Epigenomic and transcriptional determinants of microglial cell identity. Glia 68, 1643–1654. [PubMed: 31994799]
34. Feil R, Brocard J, Mascrez B, LeMeur M, Metzger D, and Chambon P (1996). Ligand-activated site-specific recombination in mice. Proc. Natl. Acad. Sci. USA 93, 10887–10890. [PubMed: 8855277]
35. Goldmann T, Wieghofer P, Jordão MJC, Prutek F, Hagemeyer N, Frenzel K, Amann L, Staszewski O, Kierdorf K, Krueger M, et al. (2016). Origin, fate and dynamics of macrophages at central nervous system interfaces. Nat. Immunol 17, 797–805. [PubMed: 27135602]
36. Haynes SE, Hollopeter G, Yang G, Kurpius D, Dailey ME, Gan WB, and Julius D (2006). The P2Y12 receptor regulates microglial activation by extracellular nucleotides. Nat. Neurosci 9, 1512–1519. [PubMed: 17115040]
37. Mastorakos P, Mihelson N, Luby M, Burks SR, Johnson K, Hsia AW, Witko J, Frank JA, Latour L, and McGavern DB (2021). Temporally distinct myeloid cell responses mediate damage and repair after cerebrovascular injury. Nat. Neurosci 24, 245–258. [PubMed: 33462481]
38. Bedolla A, Taranov A, Luo F, Wang J, Turcato F, Fugate EM, Greig NH, Lindquist DM, Crone SA, Goto J, and Luo Y (2022). Diphtheria toxin induced but not CSF1R inhibitor mediated microglia ablation model leads to the loss of CSF/ventricular spaces in vivo that is independent of cytokine upregulation. J. Neuroinflammation 19, 3. [PubMed: 34983562]
39. Turcato FC, Wegman E, Lu T, Ferguson N, and Luo Y (2022). Dopaminergic neurons are not a major Sonic hedgehog ligand source for striatal cholinergic or PV interneurons. iScience 25, 105278. [PubMed: 36281454]
40. Lagace DC, Whitman MC, Noonan MA, Ables JL, DeCarolis NA, Arguello AA, Donovan MH, Fischer SJ, Farnbauch LA, Beech RD, et al. (2007). Dynamic Contribution of Nestin-Expressing Stem Cells to Adult Neurogenesis. J. Neurosci 27, 12623–12629. [PubMed: 18003841]
41. Li L, Harms KM, Ventura PB, Lagace DC, Eisch AJ, and Cunningham LA (2010). Focal cerebral ischemia induces a multilineage cytogenic response from adult subventricular zone that is predominantly gliogenic: Ischemia Induces SVZ Gliogenic Response. Glia 58, 1610–1619. [PubMed: 20578055]
42. Jin Y, Raviv N, Barnett A, Bambakidis NC, Filichia E, and Luo Y (2015). The shh signaling pathway is upregulated in multiple cell types in cortical ischemia and influences the outcome of stroke in an animal model. PLoS One 10, e0124657. [PubMed: 25927436]
43. Zhang Z, Park JW, Ahn IS, Diamante G, Sivakumar N, Arneson D, Yang X, van Veen JE, and Correa SM (2021). Estrogen receptor alpha in the brain mediates tamoxifen-induced changes in physiology in mice. Elife 10, e63333. [PubMed: 33647234]
44. Li X, Du ZJ, Chen MQ, Chen JJ, Liang ZM, Ding XT, Zhou M, Li SJ, Li XW, Yang JM, and Gao TM (2020). The effects of tamoxifen on mouse behavior. Genes Brain Behav. 19, e12620. [PubMed: 31652391]
45. Wyatt KD, Sakamoto K, and Watford WT (2022). Tamoxifen administration induces histopathologic changes within the lungs of Cre-recombinase-negative mice: A case report. Lab. Anim 56, 297–303. [PubMed: 34551640]
46. Madisen L, Zwingman TA, Sunkin SM, Oh SW, Zariwala HA, Gu H, Ng LL, Palmiter RD, Hawrylycz MJ, Jones AR, et al. (2010). A robust and high-throughput Cre reporting and characterization system for the whole mouse brain. Nat. Neurosci 13, 133–140. [PubMed: 20023653]
47. Srinivas S, Watanabe T, Lin CS, William CM, Tanabe Y, Jessell TM, and Costantini F (2001). Cre reporter strains produced by targeted insertion of EYFP and ECFP into the ROSA26 locus. BMC Dev. Biol 1, 4. [PubMed: 11299042]
48. Larsson J, Goumans MJ, Sjöstrand LJ, van Rooijen MA, Ward D, Levéen P, Xu X, ten Dijke P, Mummery CL, and Karlsson S (2001). Abnormal angiogenesis but intact hematopoietic potential in TGF-beta type I receptor-deficient mice. EMBO J. 20, 1663–1673. [PubMed: 11285230]

49. Cheng X, Li Y, Huang Y, Feng X, Feng G, and Xiong ZQ (2011). Pulse labeling and long-term tracing of newborn neurons in the adult subgranular zone. Cell Res. 21, 338–349. [PubMed: 20938464]

50. Jin Y, Barnett A, Zhang Y, Yu X, and Luo Y (2017). Poststroke Sonic Hedgehog Agonist Treatment Improves Functional Recovery by Enhancing Neurogenesis and Angiogenesis. Stroke 48, 1636–1645. [PubMed: 28487338]

## Highlights

- For gene deletion, *Cx3cr1*$^{CreER}$ lines have the highest recombination efficiency
- For microglia labeling, *P2ry12/Tmem119*$^{CreER}$ are specific with Ai-tdTomato
- *Cx3cr1*$^{CreER(Jung)}$/*P2ry12*$^{CreER}$ do not show neonatal tamoxifen-induced inflammation
- Inter-*loxP* distance plays a key role in recombination efficiency

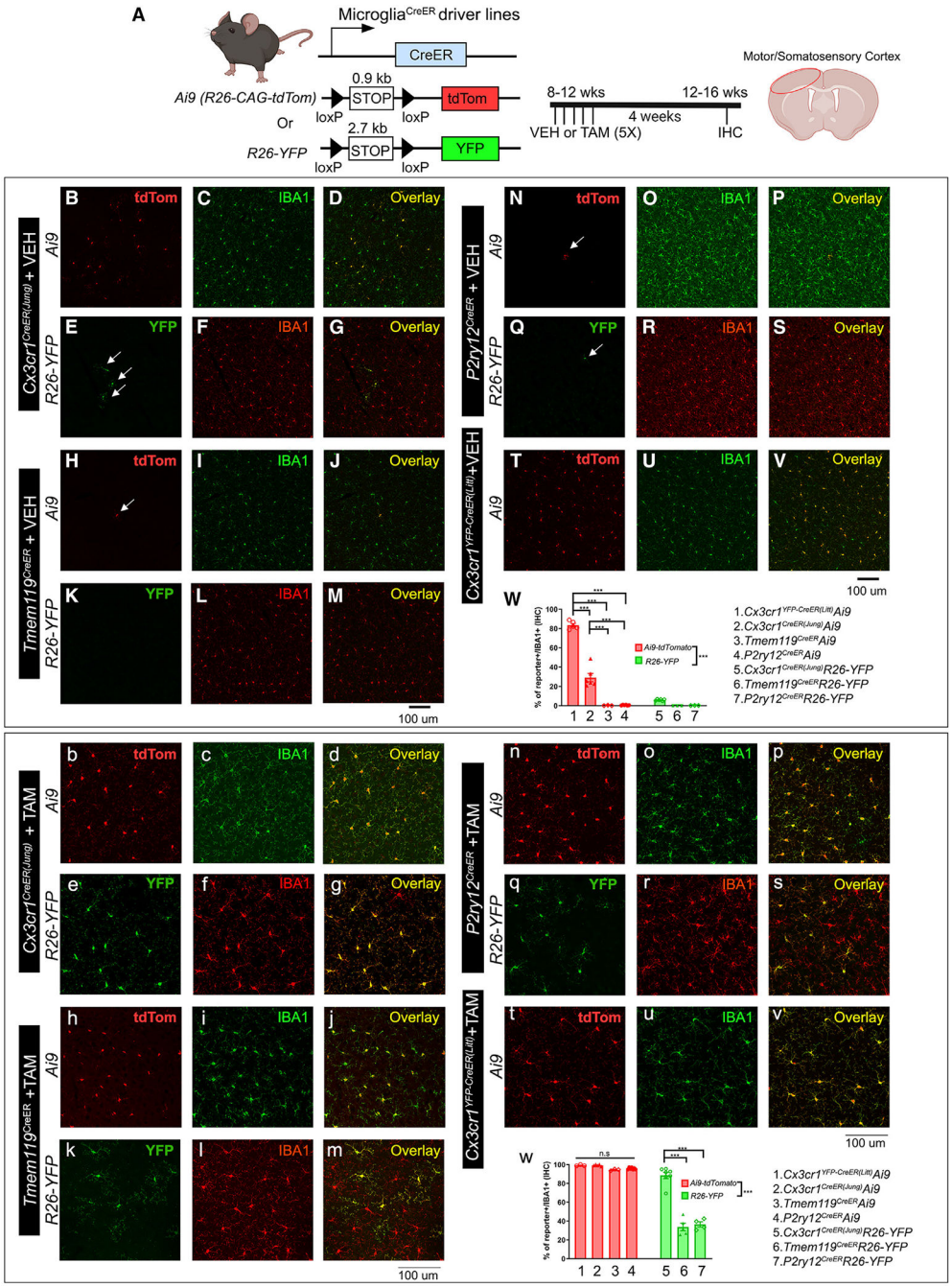


**Figure 1. Evaluation of the TAM-independent leakiness and the efficiency of TAM-dependent Cre recombination in the four different *CreER* driver lines using either the *Ai9-tdTomato* or *R26-YFP* reporter mouse lines**

The experimental timeline is shown in (A). Representative images from each *Cre* driver and reporter line are shown (B–V for vehicle [VEH] treatment and b–v for TAM treatment). The *Cre* driver and the reporter line are indicated on the left. Quantification of reporter$^{+}$ cells in the IBA1$^{+}$ populations in the brain is shown in (W) (for VEH treatment) and (w) (for TAM treatment). Representative images are taken from the cortical region, which reflects the general and homogenous trend in the whole parenchyma. Each data point represents the

average of 1 animal (the average for each animal is obtained by quantifying multiple brain sections at similar anatomical locations), and the average for each animal was used as a single data point for statistical analysis. Mean ± SEM. **p < 0.01, ***p < 0.001, two-way ANOVA, Tukey post hoc pairwise analysis. *Ai9* vs. *R26-YFP* is significantly different as a factor (p < 0.001). Data were combined from 2 independent cohorts of mice. Scale bars, 100 μm. Compared with the two *Cx3cr1*$^{CreER}$ lines (Littman and Jung), *Tmem119*$^{CreER}$ and *P2ry12*$^{CreER}$ show less leakiness in the absence of TAM but a decreased recombination efficiency and mosaic recombination in microglia. See also Figures S1-S4.

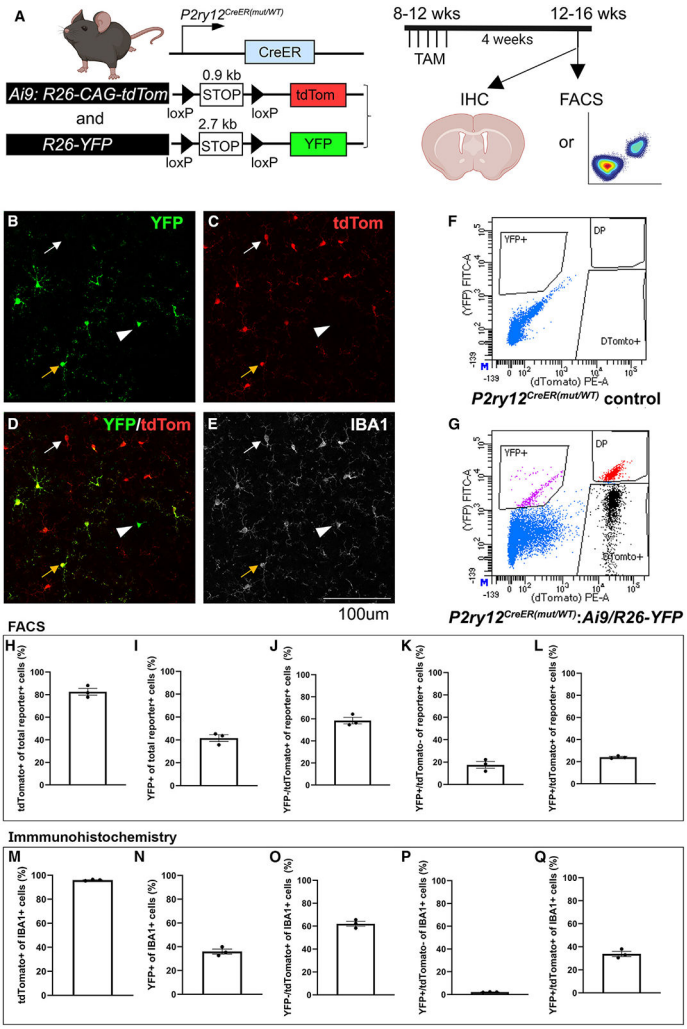


**Figure 2. Independent recombination of the two floxed alleles at the single-cell level in the *P2ry12*$^{CreER}$ double reporter (*Ai9:R26-YFP*) mouse line**

Evaluation of the TAM-dependent recombination of either the *Ai9-tdTomato* or *R26-YFP* allele, which are both located in the *R26* loci in a double reporter mouse in the *P2ry12*$^{CreER}$ line, suggests that, although, on a populational level, *Ai9-tdTomato* reporter has a higher probability of being recombined compared with the *R26-YFP* allele, at the single-cell level, the recombination of each individual allele can be independent and does not always follow the size of the floxed region rule.

(A) Experimental timeline.

(B–E) IHC evaluation of the recombination of microglia on either of the reporter expression. Note tdTomato$^{+}$:YFP$^{+}$ double-positive microglia (orange arrow), more abundant tdTomato$^{+}$:YFP$^{-}$ microglia (white arrow), and the less abundant YFP$^{+}$:tdTomato$^{-}$ microglia (white arrowhead).

(F and G) Representative FACS plots for no color control or the double reporter flow analysis.

(H–L) Graphs showing the percentage of cells based on reporter expression of total reporter$^{+}$ cells from FACS-sorted double-positive cells; each data point is from a single FACS sample from a single animal.

(M–Q) Graphs showing the percentage of cells based on reporter expression of total IBA1$^{+}$ cells sampled from IHC on the cortex; each data point is the average of 3 sampled images from a single animal.

Mean ± SEM. Scale bar, 100 μm. See also Table S1.

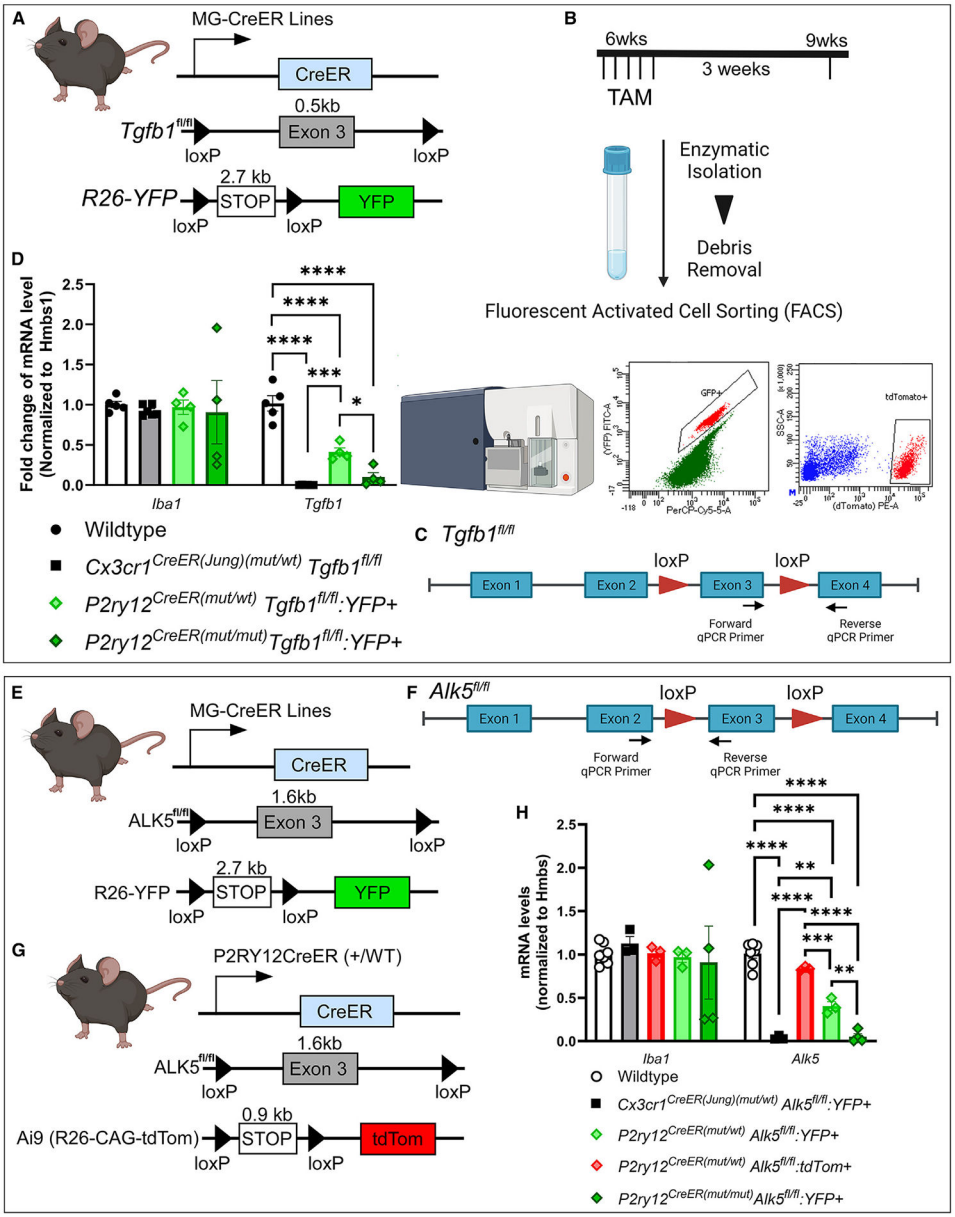


**Figure 3. Evaluation of the gene deletion efficiency on distinct homozygous floxed target gene alleles in the *Cx3cr1*$^{CreER(Jung)}$ and *P2ry12*$^{CreER}$ drivers using real-time qPCR**

(A–D) Animal genotype and experimental flow. Total mRNA levels are evaluated for the floxed exon in the *Tgfb1* gene in YFP$^{+}$ microglia sorted from the *Cx3cr1*$^{CreER(Jung)(mut/WT)}$, *P2ry12*$^{CreER(mut/WT)}$*Tgfb1*$^{fl/fl}$*R26-YFP*, or *P2ry12*$^{CreER(mut/mut)}$*Tgfb1*$^{fl/fl}$*-R26-YFP* mice 3 weeks after TAM treatment. YFP$^{+}$ cells were selected based on fluorescein isothiocyanate (FITC) wavelength to detect YFP and PerCP-Cy5.5 to help delineate the actual YFP signal from autofluorescence commonly seen in sorted brain cells.

(E–H) Total mRNA levels are evaluated for the floxed exon in the *Alk5* gene in either YFP$^{+}$ microglia sorted from the *Cx3cr1*$^{CreER(Jung)(mut/WT)}$, *P2ry12*$^{CreER(mut/WT)}$*Alk5*$^{fl/fl}$*R26-YFP*, or *P2ry12*$^{CreER(mut/mut)}$*Alk5*$^{fl/fl}$*-R26-YFP* mice or *Ai9*-tdTomato$^{+}$ microglia from the *P2ry12*$^{CreER(mutt/WT)}$*Alk5*$^{fl/fl}$*Ai9* mice 3 weeks after TAM treatment.

Each data point represents the average of 1 animal (the average for each animal is obtained by averaging 3 technical replications of the real-time qPCR reaction for that animal), and the average for each animal was used as a single data point for statistical analysis. Mean ± SEM. **p < 0.01, ***p < 0.001, ****p < 0.0001 for two-way ANOVA, Tukey post hoc pairwise analysis. Data are pooled from samples sorted either with or without transcriptional and translational inhibitors. Our data show that no difference was observed in *Tgfb1* gene or *Alk5* gene expression in sorted microglia with or without the inhibitors (see Figure S5). Also, see Figure S6 for no changes in *Tgfb1* or *Alk5* mRNA in VEH-treated mice.

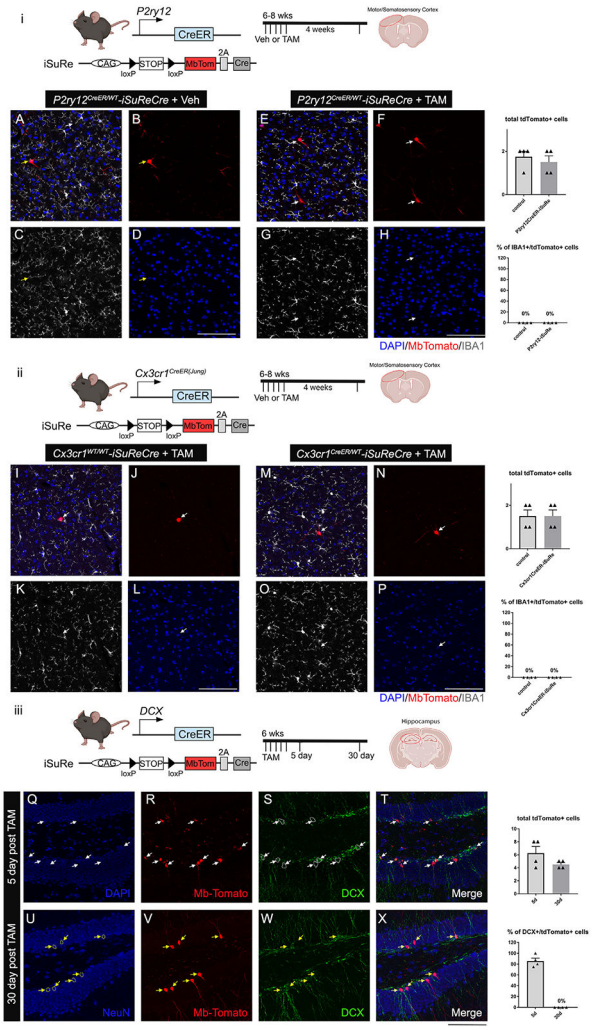


**Figure 4. The *iSuReCre* mouse line successfully induces constitutive *Cre-P2A-MbTomato* expression in the *DCX*$^{CreER}$ mouse line, but not in the *P2ry12*$^{CreER}$ or *Cx3cr1*$^{CreER(Jung)}$ mouse line, after TAM treatment**

(i) Illustration of *P2ry12*$^{CreER}$ mouse transgene constructs and experimental timeline.

A–D) In the absence of TAM, there is no MbTomato expression in microglia with ectopic MbTomato expression in cells that demonstrate typical neuron morphology in the cortex and striatum (yellow arrow, mbTomato cell).

(E–H) Treatment of TAM in mice does not induce MbTomato expression in microglia and presents with similar neuronal ectopic expression of MbTomato.

(ii) Illustration of *Cx3cr1*$^{CreER(Jung)}$ mouse transgene constructs and experimental timeline.

(I–L) In the absence of TAM, there is a pattern similar to the *P2ry12*$^{CreER}$ line.

(M–P) Treatment of TAM in mice does not induce MbTomato expression in microglia and presents with similar neuronal ectopic expression of MbTomato.

(Q–X) In contrast, in the *DCX*$^{CreER}$*-iSuReCre* mice treated with TAM, 5 days post TAM treatment, DCX$^{+}$ immature neuroblasts are labeled with MbTomato protein (white arrows), and 30 days post TAM treatment, MbTomato expression is mostly detected in DCX$^{-}$NEUN$^{+}$ mature neurons (yellow arrows), supporting that the *iSuReCre* construct is able to be

induced in a cohort of immature neuroblasts that mature later into $NeuN^+$ neurons in the dentate gyrus of adult mice.

Mean ± SEM. Scale bar, 100 μm.

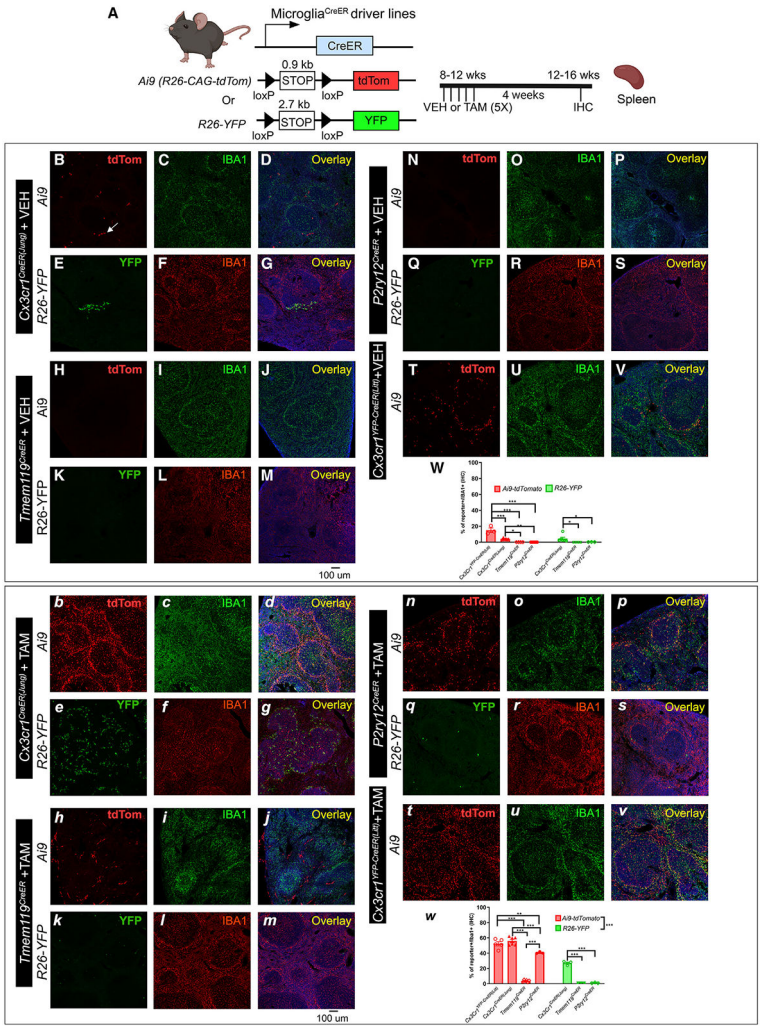


**Figure 5. Evaluation of the splenic TAM-independent and TAM-dependent *Cre* recombination in the four different *CreER* driver lines using either the *Ai9-tdTomato* or *R26-YFP* reporter mouse lines**

The experimental timeline is shown in (A). Representative images from each Cre driver and reporter line (B–V for VEH treatment and b–v for TAM treatment). The *Cre* driver and the reporter line are indicated on the left. Quantification of reporter$^+$ cells in the IBA1$^+$ populations in the spleen is shown in (W) (for VEH treatment) and (w) (for TAM treatment). Each data point represents the average of 1 animal (the average for each animal is obtained by quantifying multiples spleen sections), and the average for each animal was used as a single data point for statistical analysis. Mean ± SEM. **p < 0.01, ***p < 0.001, two-way ANOVA, Tukey post-hoc pairwise analysis. *Ai9* vs. *R26-YFP* is significantly different as a factor (p < 0.001 for the TAM-treated group). Data were combined from 2–3 independent cohorts of mice. Scale bar, 100 μm.

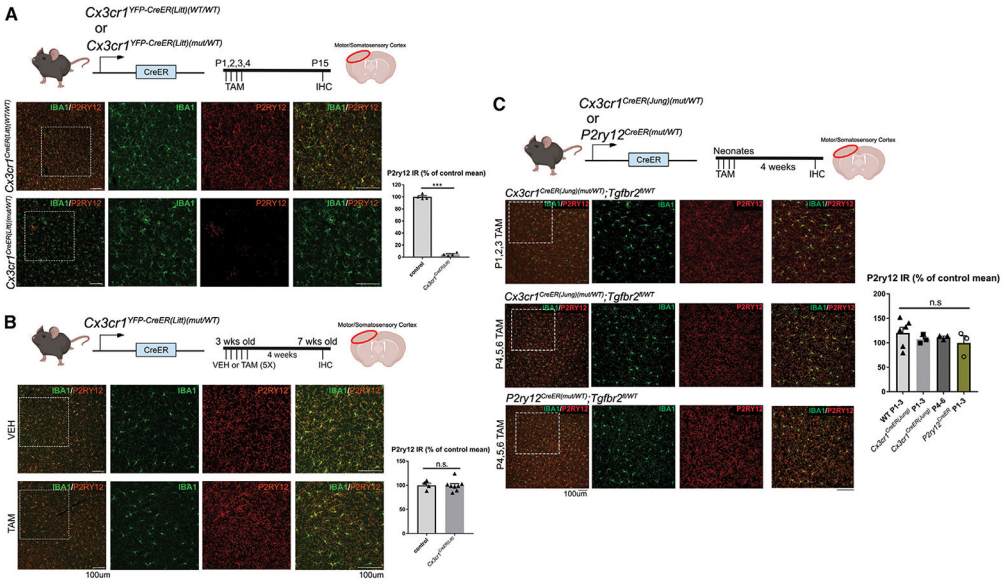


**Figure 6. Evaluation of the dyshomeostatic microglia in different microglia-specific *CreER* drivers after TAM treatment at different ages**

P2RY12 expression is used as a measure of dyshomeostasis in microglia.

(A) Consistent with previous studies, we observe dyshomeostasis of microglia (indicated by loss of P2RY12 expression) across many regions in the neonatal *Cx3cr1*$^{CreER(Litt)(mut/WT)}$ mice treated with TAM.

(B and C) This phenotype is not observed in (B) the adolescent (3-week-old) *Cx3cr1*$^{YFP\text{-}CreER(Litt)(mut/WT)}$ mice that received TAM treatment or (C) neonatal *Cx3cr1*$^{CreER(Jung)(mut/WT)}$ and P2*ry12*$^{CreER\ (mut/WT)}$ mice that received TAM on early neonatal days.

Quantifications of P2RY12 immunoreactivity are shown in the bar charts next to the representative images for each line. Mean ± SEM. Scale bars, 100 μm.

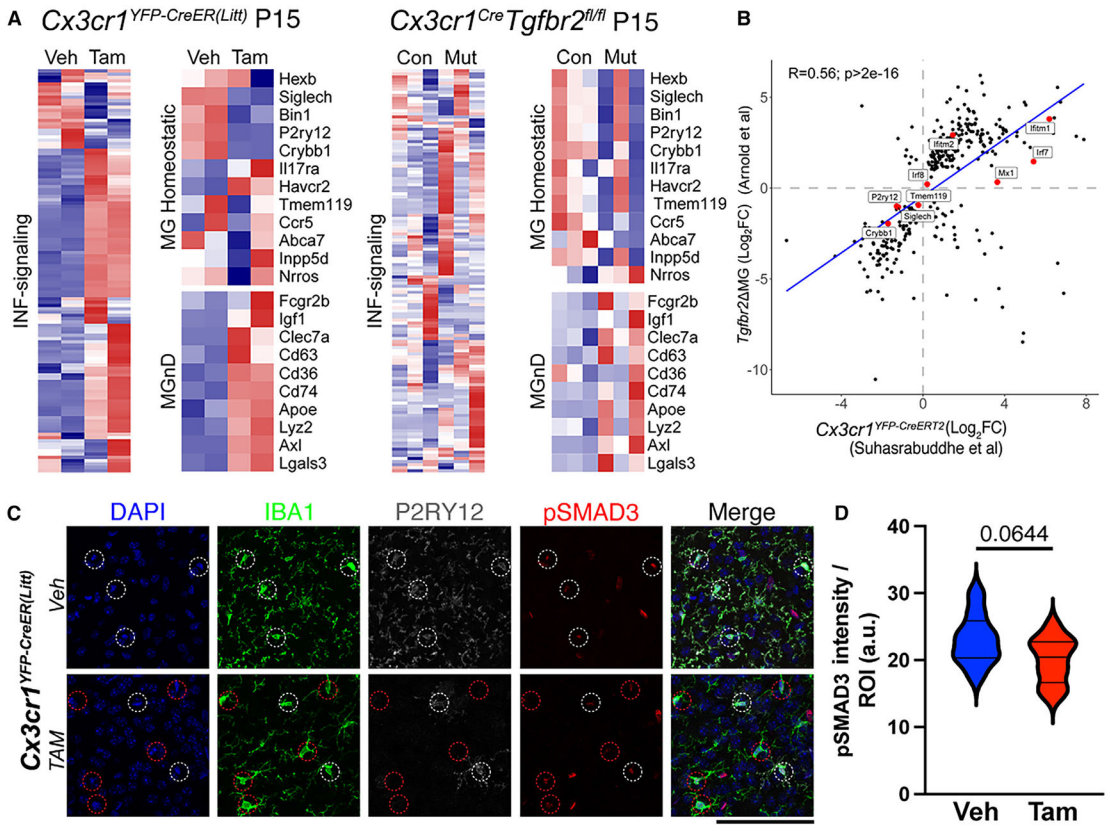


**Figure 7. Similarity in microglia phenotypes from neonatal TAM -induced *Cx3cr1*$^{YFP\text{-}CreER(Litt)}$ and *Tgfbr2*$^{fl/fl}$;*Cx3cr1*$^{Cre}$ mice**

(A) Transcriptomic phenotypes from P15 *Cx3cr1*$^{CreER(Litt)}$ (VEH vs. TAM) and *Tgfbr2;Cx3cr1*$^{Cre}$ (*Tgfbr2*$^{fl/WT}$;Cre vs. *Tgfbr2*$^{fl/fl}$;Cre) mice showing changes in INF signaling-related, MgND/DAM, and homeostatic gene expression.

(B) Correlation between two datasets.

(C) Brain sections from P15 *Cx3cr1*$^{CreER(Litt)}$ (VEH vs. TAM) mice stained for DAPI (blue), IBA1 (green), P2RY12 (gray), and pSMAD3 (red).

(D) Quantification of pSMAD3 mean fluorescence intensity in individual microglia from each group shows no significant difference in pSMAD3 (mean ± SEM, p = 0.0644, Student's t test). A red circle in (C), bottom row, indicates the P2RY12$^{-}$ microglia. Data were combined from 3 VEH-treated and 4 TAM-treated mice. Scale bars, 100 μm.

**Table 1.**

Summary of key features across different microglia CreER driver lines in adulthood

| Mouse line | TAM dose | Administration method | Collection time point (post TAM) | Brain regions examined | Specificity | Leakiness | Efficiency | Extraneural recombination | | Off-target effects | Use information | |
|---|---|---|---|---|---|---|---|---|---|---|---|---|
| | | | | | | | | Blood | Spleen | | Availability | Reference |
| *Cx3cr1*$^{YFP\_CreER(Litt)}$ | 10 mg (2x) | oral gavage | P5/P30 | motor CTX | + | +++ | +++ | ++ | +++ | +++ | JAX: 021160 | Parkhurst et al.[17] |
| | 180 mg/kg (5x) | | 4 weeks | motor CTX, STR, HC | | | | | | | | |
| *Cx3cr1*$^{CreER(Jung)}$ | 400 mg/kg | subcutaneous | 3 weeks/8 weeks | ehole brain | + | ++ | ++ | ++ | ++ | + | JAX: 020940 | Yona et al.[18] |
| | 180 mg/kg (5x) | oral gavage | 4 weeks | motor CTX, STR, HC | | | | | | | | |
| *P2ry12*$^{CreER}$ | 3 mg (3x) | oral gavage | ? | spinal cord, cerebellum, CTX, HC | ++ | + | + | − | + | − | JAX: 034727 | McKinsey et al.[8] |
| | 180 mg/kg (5x) | | 4 weeks | motor CTX, STR, HC | | | | | | | | |
| *Tmem119*$^{CreER}$ | 0.2 mg/g (3x) | oral gavage | P3–P10 | somatosensory CTX, STR, HC, thalamus, ChP | ++ | + | + | − | − | − | JAX: 031820 | Kaiser et al.[10] |
| | 180 mg/kg (5x) | | 4 weeks | Motor CTX, STR, HC | | | | | | | | |
| *HexB*$^{CreER}$ | 4 mg (2x), 6 mg (3x) | intraperitoneal (i.p.) | P5 | olfactory bulb, CTX, HC, cerebellum, spinal cord | +++ | + | + | +++ | ++ | + | not publicly available | Masuda et al.[9] |
| *Sall1*$^{CreER}$ | 2.5 mg (5x) | i.p. | P0–P14 | CTX, HC, cerebellum, thalamus | + | ++ | + | − | ? | + | not publicly available | Buttgereit et al.[15] |

**Table 2.**

Summary of findings from various mouse lines in developmental and neonatal mice

| *Cre/CreER* line | Developmental time point induced | Time analyzed | Reference | TAM dose | Reporter | Recombination efficiency | Observations |
|---|---|---|---|---|---|---|---|
| *Cx3cr1*$^{YFP\text{–}CreER(Litt)}$ | P3–P5 | P7–P9 | Sahasrabuddhe and Ghosh[14] | 50 μg (IG) | none | not reported | artifactual production of reactive microglia in a *CreER*- and TAM-dependent fashion |
| *Cx3cr1*$^{CrerER\ (Jung)}$ | P1, P2, P3 | P7, P30, P120 | Arnold et al.[30] | 1 mg/mL (50 μL) (IG) | *Ai14: tdTomato* | 95% | lower penetrance of T*gfbr2* recombination; microglia and BAMs are specifically recombined; no artifactual reactive microglia observed |
| *Tmem119*$^{CreER}$ | P2, P3, P4 | P14 | Kaiser et al.[10] | 20 mg/mL (5 μL) (IG) | *Ai14: tdTomato* | cortex, 90%–100%; caudate putamen, 96%–100%; hippocampus, 94%–100% | endothelial recombination in addition to macrophages; potential mural cell recombination |
| *P2ry12*$^{CreER}$ | Embryonic day 13.5 (E13.5)–E17.5 | E18.5 | McKinsey et al.[8] | 20 mg/mL (150 μL) oral gavage | *Ai14: tdTomato* | not reported | widespread recombination of microglia; low pial macrophage recombination (8%–12%); potential recombination in microglial precursors |

## KEY RESOURCES TABLE

| REAGENT or RESOURCE | SOURCE | IDENTIFIER |
|---|---|---|
| Antibodies | | |
| Goat Iba1 antibody | Abcam | Cat# ab5076; RRID: AB_2224402 |
| Rat P2RY12 antibody | BioLegend | Cat#848002; RRID: AB_2650634 |
| Rabbit anti-Mouse P2RY12 antibody | AnaSpec | Cat#55043A; RRID: AB_2298886 |
| Rabbit anti-Green Fluorescent Protein (GFP) Polyclonal Antibody | Invitrogen | Cat#A11122; RRID: AB_221569 |
| Recombinant Anti-Smad3 (phospho S423 + S425) antibody (1:200, host: rabbit) | Abcam | Cat# ab52903; RRID: AB_882596 |
| DCX (1:1000, host: rabbit) | Cell Signaling | Cat#4604s |
| LYVE1 (1:600, host: rabbit) | Abcam | Cat#ab14917; RRID: AB_301509 |
| CD206 (1:200, host: rat) | Biorad | Cat#mca2235; RRID: AB_324622 |
| Donkey anti-Goat IgG (H + L) Highly Cross-Adsorbed Secondary Antibody, Alexa Fluor™ Plus 488 | Thermo Fisher Scientific | Cat# A32814; RRID: AB_2762838 |
| Donkey anti-Goat IgG (H + L) Cross-Adsorbed Secondary Antibody, Alexa Fluor™ 555 | Thermo Fisher Scientific | Cat# A-21432; RRID: AB_2535853 |
| Cy3-AffiniPure Donkey Anti-Rat IgG (H + L) | Jackson ImmunoResearch | Cat# 712-165-153; RRID: AB_234066 |
| Alexa Fluor 647-AffiniPure Donkey Anti-Rat IgG (H + L) | Jackson ImmunoResearch | Cat# 712-605-153; RRID: AB_2340694 |
| Cy3-AffiniPure Donkey Anti-Rabbit IgG (H + L) | Jackson ImmunoResearch | Cat#715-165-152 |
| Alexa Fluor 647-AffiniPure Donkey Anti-Rabbit IgG (H + L) | Jackson ImmunoResearch | Cat# 711-605-152; RRID: AB_2492288 |
| Chemicals, peptides, and recombinant proteins | | |
| Tamoxifen | Sigma | T5648-5G |
| Sunflower seed oil | Sigma | S5007 |
| 100% Ethanol | Sigma | 493546-1L |
| Percoll | GE | 17-0891-01 |
| 10x HBSS | Thermo Fisher Scientific | 14185052 |
| 1x HBSS | Thermo Fisher Scientific | 14175079 |
| DAPI | Sigma | D9542 |
| DNaseI | Roche | 10104159001 |
| Bovine Serum Albumin | Sigma | 9048-46-8 |
| Normal Donkey Serum | Jackson ImmunoResearch | 017-000-121 |
| Triton-100x | Sigma | T8787 |
| Critical commercial assays | | |
| Papain dissociation kit | Worthington | Cat#LK003150 |
| RNAqueous™-Micro Total RNA Isolation Kit | ThermoFisher | Cat#AM1931 |
| iScript cDNA Synthesis Kit | BioRad | Cat#1708890 |
| TaqMan fast advanced master mix | ThermoFisher | Cat#4444556 |
| Tgfbr1 qrtPCR assay (Mm00436965_m1) | ThermoFisher | Cat#4351372 |
| Tgfb1 qrtPCR assay (Mm03024053_m1) | ThermoFisher | Cat#4331182 |
| Roche Universal Probe Library #79 | Roche | Cat# UPL71THRU80 |
| Roche Universal Probe Library #108 | Roche | Cat# UPL101THRU110 |

| REAGENT or RESOURCE | SOURCE | IDENTIFIER |
|---|---|---|
| Roche Universal Probe Library #3 | Roche | Cat# UPL1THRU10 |
| Deposited data | | |
| (*Cx3cr1*$^{CreER}$ Littman) + TAM RNA-seq | Sahasrabuddhe and Ghosh[14] | GEO: GSE190207 |
| (*Tgbfr2 fl/fl;Cx3cr1*$^{Cre}$at P15) RNA-seq | Arnold et al.[30] | GEO: GSE124868 |
| Experimental models: Organisms/strains | | |
| Mouse: B6.129P2(Cg)-Cx3cr1tm2.1(cre/ERT2)Litt/WganJ | The Jackson Laboratory | IMSR Cat# 021160; RRID: IMSR_JAX:021160 |
| Mouse: B6.129P2(C)-Cx3cr1tm2.1(cre/ERT2)Jung/J | The Jackson Laboratory | IMSR Cat# 020940; RRID: IMSR_JAX:020940 |
| Mouse: B6(129S6)-P2ry12em1(icre/ERT2)Tda/J | The Jackson Laboratory | IMSR Cat# 034727; RRID: IMSR_JAX:034724 |
| Mouse: C57BL/6-Tmem119em1(cre/ERT2)Gfng/J | The Jackson Laboratory | IMSR Cat# 031820; RRID: IMSR_JAX:031820 |
| Mouse: B6.Cg-Gt(ROSA)26Sortm9(CAG-tdTomato)Hze/J | The Jackson Laboratory | IMSR Cat# 007909; RRID: IMSR_JAX:007909 |
| Mouse: B6.129X1-Gt(ROSA)26Sortm1(EYFP)Cos/J | The Jackson Laboratory | IMSR Cat# 006148; RRID: IMSR_JAX:006148 |
| Mouse: STOCK Tgfbr1tm1.1Karl/KulJ | The Jackson Laboratory | IMSR Cat# 028701; RRID: IMSR_JAX:028701 |
| Mouse: C57BL/6J-Tgfb1em2Lutzy/Mmjax | The Jackson Laboratory | IMSR Cat# 065809-JAX; RRID: MMRRC_065809-JAX |
| Mouse: DCXCreER | Gift from Dr. Zhi-qi Xiong, Chinese academy of sciences | MGI: 5438982 (Not commercially available) |
| Mouse: iSuReCre | Gift from Dr. Rui Benedito, CNIC, Spain | Fernández-Chacón et al.[19] (Not commercially available) |
| Oligonucleotides | | |
| Primers: Hbms (Probe #79)<br>F: TCC CTG AAG GAT GTG CCT AC | Integrated DNA Technologies | N/A |
| Primers: Hbms (Probe #79)<br>R: ACA AGG GTT TTC CCG TTT G | Integrated DNA Technologies | N/A |
| Primers: PGK1 (Probe #108)<br>F: TAC CTG CTG GCT GGA TGG | Integrated DNA Technologies | N/A |
| Primers: PGK1 (Probe #108)<br>R: CAC AGC CTC GGC ATA TTT CT | Integrated DNA Technologies | N/A |
| Primers: Iba1 (Probe #3)<br>F: GGA TTT GCA GGG AGG AAA A | Integrated DNA Technologies | N/A |
| Primers: Iba1 (Probe #3)<br>R: TGG GAT CAT CGA GGA ATT G | Integrated DNA Technologies | N/A |
| Software and algorithms | | |
| ImageJ | https://ImageJ.nih.gov/ij/ | https://doi.org/10.1038/nmeth.2089 RRID:SCR_003070 |
| Nikon Element | Nikon | V3.22; RRID: SCR_014329 |
| Stereo Investigator Image Software | MBF Bioscience | V2022.2.1; RRID:SCR_002526 |
| Other | | |
| Microscope | Leica | DM5000B |
| Confocal Microscope | Leica | Stellaris 8 |
| FACS | BD Biosciences | BD/FACSAria II |